Article:

Cardoso de Freitas Murari, M, de Hollanda Cavalcanti Tsuha, C and Loveridge, F orcid.org/0000-0002-6688-6305 (2022) Investigation on the thermal response of steel pipe energy piles with different backfill materials. Renewable Energy, 199. pp. 44-61. ISSN 0960-1481

https://doi.org/10.1016/j.renene.2022.08.105

Abstract

The use of geothermal energy piles (GEPs) associated with ground source heat pump systems is a sustainable and cost effective technology to heat and cool buildings, based on the efficient application of available resources found at the building site. Currently, a new building with GEPs is under construction at the University of São Paulo campus in São Paulo City, Brazil. Part of the building loads will be supported by steel pipe piles equipped with single U-type absorber pipes for heat exchange. To find the optimum solution of pile backfill material in terms of cost, constructability, sustainability and thermal performance, field thermal response tests were conducted on 4 instrumented piles filled with different materials: water, saturated sand, grout, and steel fiber grout. Both analytical and numerical models were used to evaluate the tested alternatives. The results showed that the thermal performance of the 4 piles is similar; however, the costs and sustainability aspects (low CO2 emissions) of the solutions using water or saturated sand imply that they are more advantageous than those using grout. Additionally, the experiments showed that for the pile backfilled with water the convection effects have improved the heat transfer to the soil.

Keywords: geothermal energy piles (GEP), steel pipe piles, field thermal response test, analytical methods, numerical analysis.

ABBREVIATION LIST

AR – Aspect ratio

CFA - Continuous flight auger

CICS - Center for innovation in sustainable construction

CO2 - Carbon dioxide

EPE – Empresa de Pesquisa Energética (Energy research company translated from portuguese)

GEP - Geothermal energy pile

GHE – Ground heat exchanger

GSHP – Ground source heat pump

HDPE - High density polyethylene pipe

HBM - Hottinger Baldwin Messtechnik

ILSM – Infinite Line Source Model

RMSE – Root mean square error

SCSM – Solid Cylinder Source Model

TRT - Thermal response test

NOMENCLATURE LIST

$C_{p,m}$ = *specific heat of water medium (J/ KgK)*

C_{pc} = *backfill material specific heat capacity (J/kgK)*

C_{pf} = *fluid specific heat capacity (J/kgK)*

C_{pg} = *ground specific heat capacity (J/kgK)*

d_o = *outer pipe diameter (m).*

F_0 = *Fourier number*

G_c = *G-functions for the concrete temperature responses*

G_g = *G-functions for the ground temperature responses*

H = *GHE length (m)*

h_i = *convective heat transfer coefficient* $(W/(m^2K)$

k_m = *thermal conductivity of the medium in (W/mK)*

k_p = *thermal conductivity of the pipe (W/mK)*

m = *mass flow rate (kg/s)*

n = *number of pipes within the pile*

N_u = *Nusselt number*

Θ_c = *temperature rise at the heat source*

q = *applied heat power (W/m)*

Q = *Heating Power (W)*

Q_{wall} = *heat transferred by the tube wall (W)*

R_b =*Pile thermal resistance (mK/W)*

r_i = *pipe internal radius*

R_p = *Pipe thermal resistance (mK/W)*

$R_{p\ cond}$ = *Conduction pipe thermal resistance (mK/W)*

$R_{p\ convec}$ = *Convective pipe thermal resistance (mK/W)*

T = *temperature (K)*

t = *time (s)*

T_{in} = *Inlet temperature (K)*

T_{out} =*Outlet temperature (K)*

T_{w2} = *temperature outside the pipe (K)*

u = *fluid velocity (m/s)*

α_g= *ground thermal diffusivity* (m^2/s)

ΔT_g = *Ground temperature variation (°C)*

λ = *effective thermal conductivity (W/mK)*

λ_c =*Backfill material thermal conductivity (W/mK)*

λ_g = *Ground thermal conductivity (W/mK)*

ρC_p = *the volumetric heat capacity* ($J/m^3/K$)

ρ_m = *water density* (kg/m^3)

Φ = *normalized temperature*

1. Introduction

Energy demand for space cooling purposes accounts for 6% of the global energy used in buildings, and this number is growing rapidly worldwide as the installation of air conditioners is increasing every year [1] Moreover, global climate change impacts local weather conditions with consequences for energy consumption in buildings [2].

In Brazilian commercial buildings, air-conditioning systems represent 30 to 40 percent of the total building energy consumption [3]. For residential purpose, according to the EPE [4], the power consumption associated with air conditioners has more than tripled in Brazil between 1990 and 2018. Besides this increased demand for artificial cooling, the impacts of climate change on the Brazilian hydroelectric power plants operation has affected the price of energy [5]. This highlights the urgent need of exploitation of new sources of clean energy in Brazil and other countries. To alleviate this critical issue, the use of shallow geothermal energy can be a sustainable alternative for thermal comfort of buildings. However, this source of thermal energy is not yet exploited in Brazil due to an absence of reported cases in the literature and in the practice to demonstrate the feasibility of these systems in appropriate local climate and ground conditions.

Shallow geothermal energy is a renewable energy solution for building thermal control which is traditionally employed using horizontal ground heat exchangers or deep boreholes heat exchangers. This type of energy can also be exploited from deep foundations, that are already in the ground for structural support. The use of foundations as ground heat exchangers can provide both material and carbon savings compared with the construction of deep boreholes [6].

Foundation piles integrated with absorber pipes filled with a heat carrier fluid, known as geothermal energy piles (GEP), take advantage of the thermal storage capacity of the ground, and are an environmental friendly way of heating and cooling buildings [7]. Heat transfer in energy piles occurs by means of conduction and convection. Conduction dominates heat transfer in solid materials and convection is the mode of heat transfer of moving fluids [8].

Although the installation cost for ground heat exchangers providing an incentive for the use of GEPs, in some cases additional cost to the building foundation is needed. For example, for concrete piles, additional steel bars may be required to accommodate the absorber pipes, or additional programme time needed in construction. For the case of concrete or steel pipe energy piles, these may need to be filled with additional materials like concrete or grout. While thermo-activation does not typically require changes to the pile design, all GEPs should also be checked for structural implications of the resulting temperature changes [8].

The Brazilian needs for sustainable cooling described above were the motivation for the implementation of geothermal energy piles for space cooling of a building in São Paulo city, in the southeast Region of Brazil (annual average temperature of ~ 19.3-19.6 °C). This building under construction, which is part of the CICS Living Lab of the University of Sao Paulo, will be supported by continuous flight auger (CFA) and steel pipe piles, equipped with U-shaped pipes, installed in a saturated sandy deposit interbedded with thin soft clayey layers. The use of ground source heat pumps (GSHP) with multiple energy piles have been used in other countries since the 1980's [9], and has increased over the years, especially in Europe and in the United States. However, there are no reports of GEP cases in Brazil.

To help in decision making on the most suitable filling material for the steel pipe GEPs to be used for the CICS building, in situ thermal response tests (TRTs) were conducted to compare the thermal performance of steel pipe energy piles filled with 4 different materials: water, saturated sand, grout, and steel fiber grout. This paper presents the work carried out to help choose the most appropriate pile backfilled material in terms of cost, thermal performance, constructability, and sustainability (CO2 emissions).

Although there are some studies that evaluated pipe energy piles filled with different materials such as grout or concrete [10,11], sand [12], and water [13,14,15,16], it is rare for studies to have compared the effect of different backfill materials on the thermal performance of pipe energy piles under identical geometrical and ground conditions. Among these rare cases, Cao et al. [17] presented a study on the influence of different backfill materials (ordinary grout, Phase Change Materials (PCM), enhanced-PCM, and water) on the heat exchange rate of pipe energy piles. However in this case they tested concrete energy piles, whereas the current study is focused on steel pipe energy piles and the effects of filling material on the pile thermal resistance (not evaluated in Cao et al. [17].

The main novelties and contributions of this study are to: (i) provide field results on the heat transfer behaviour of steel pipe energy piles and their evaluation using analytical and numerical approaches, which are rarely found in the literature; (ii) present experimental data to improve the design of future energy piles to be operated in Brazilian conditions; (iii) show the effect of the filling material on the energy pile performance; (iv) provide quantitative information on the heat transfer efficiency of four different filling materials for hollow steel energy piles of same geometry in identical soil conditions; (v) provide novel insights into the mechanisms that improve the heat transfer for piles filled with water, which is the more economical and environmental-friendly alternative for energy pile filling material; (vi) show that low-cost and sustainable filling materials such as sand or water can be feasible alternatives for the use of steel pipe piles to be used as energy geoestructures.

Delivering on these contributions, the paper is set out in the following way. In Section 2, the pile construction, instrumentation and thermal response testing is described in detail. Section 3 presents the methods used to interpret the thermal response tests, including a range of analytical and numerical techniques in two and three dimensions. In Section 4, the results of the field tests are shown and the fit of the analytical and numerical models is presented and discussed. The fitted model parameters are used to determine the thermal resistance of the piles with the different filling materials and these are compared in Section 5. Cost of construction data is also considered alongside thermal performance (in terms of thermal resistance), allowing conclusions to be presented in Section 6.

2. Experimental program

2.1. Test piles

The current experimental study was carried out at the site of the CICS Living Lab, a building under construction at the campus of the University of São Paulo, in the urbane zone of São Paulo city, Brazil. Steel pile piles with an external diameter of 244 mm and wall thickness of 10 mm were driven to a depth of ~ 23 m (Fig. 1a) to compose the foundation of a part of the building. Four additional closed-ended piles (Fig. 1b) were installed at the same site for the evaluation of the pile thermal performance using different pile backfill material.

Figure 1. Installation of the test energy piles: (a) pile installation; (b) closed end test pile; (c) pile instrumentation; (d) single U-tube; (e) installation of U-shaped pipes into the pile foundation.

Generally, conventional steel pipe piles used only for structural/geotechnical purposes are not filled. In specific cases they are filled with concrete to improve the strength and capacity under lateral loading [26]. However, when pipe piles are employed as energy geostructures for the exploitation of shallow geothermal energy, they are typically filled with concrete [9,11], grout [17,27], water [13, 28, 29, 30, 31], or sand [12] to ensure the heat transfer between the pipes and the ground during the GSHP operation.

The use water or sand as pile filling material is more economical compared to the use of concrete or grout. Additionally, as no cement is required for these cases, they also provide reduced CO2 emissions. For energy pipe piles with sand as a filling material, the heat transfer performance is better when the sand is saturated, as observed from reduced-scale model tests in Murari [32]. The use of steel pipe energy piles filled with saturated sand or water in areas with high level of groundwater may be simpler to control. Therefore, where the ground conditions are suitable for pile driving, and where the environment can tolerate the noise and vibration caused by driving [33], energy pipe piles are a good solutions. In the case investigated here, the test piles were installed in an area with no nearby buildings at the campus of the University of São Paulo. Generally, to minimize noise and vibration associated with the piling work, rotary jacking methods [33-36] are recommended for steel pile installation.

The four test piles were equipped with a single U-tube of high-density polyethylene (HDPE) pipe with inner diameter of 26 mm and outer diameter of 32 mm (PE 100 SDR 11). The pipes were installed manually into the piles using plastic spacers (Figs. 1c-e) to prevent pipe thermal interactions. The test piles were instrumented with platinum thermistor sensors, PT 100 class A, with an accuracy of ±0,15 for 0°C and ±0,35 for 100°C. The sensors were attached to a steel bar fixed in the centre or in the edge of plastic spacer, as shown in Fig.1c. The depth of temperature sensors were chosen in order to provide temperature variation along the pile at different layers of the soil profile. After pipe installation (Fig. 2a), the test piles were backfilled with different materials: water, saturated sand, grout, and steel fiber grout (Fig. 2).

The pile P1 was filled with water, and the pile P2 with coarse grey sand (saturated after the filling process), as illustrated in Figs. 2b-c. For the pile P3, a cement-sand grout was used as backfill material (Fig. 2d). The mixture was composed of 200 kg of cement, 1627 kg of sand and a water/cement ratio of 1.4 for each cubic meter of grout. For the pile P4, filled with steel fiber grout (Fig. 2e), 30 kg of steel fibers were added to each 1 m^3 of grout. The materials were mixed using a mixer truck (Figs. 2d-e). Steel fibers of 0.62 mm diameter and 35 mm long (DRAWMIX fiber, fabricated by ArcelorMittal) were used in this study (Fig. 2f).

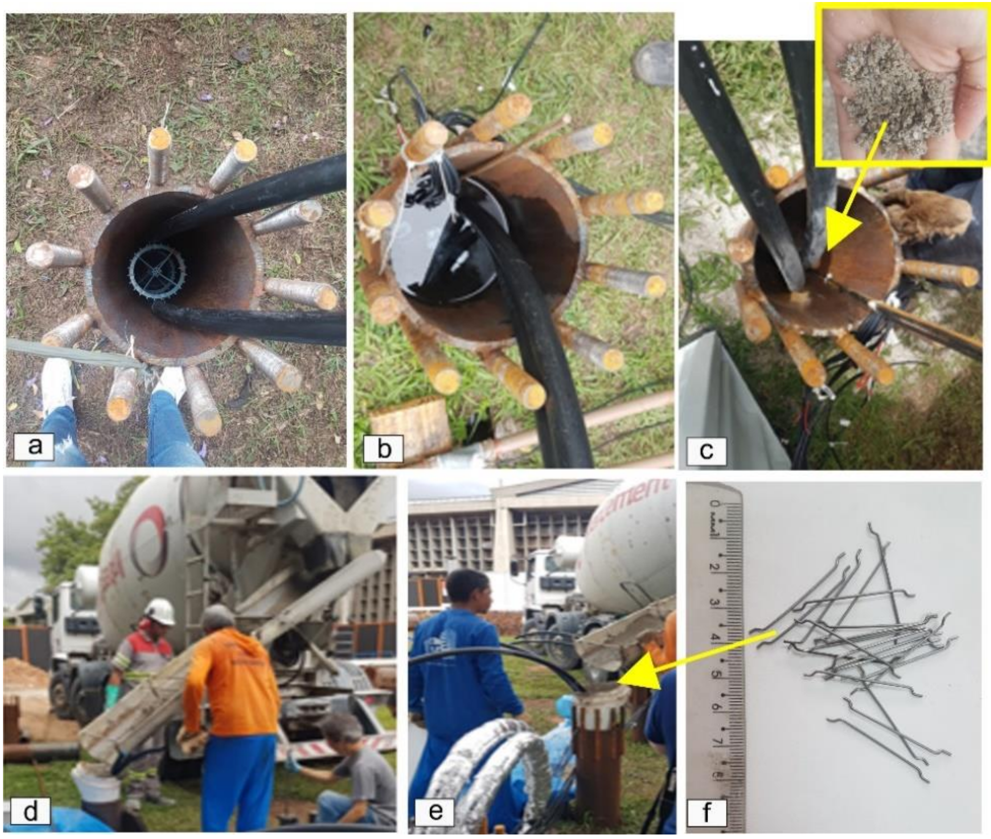

Figure 2. (a) Test pile before filling process; (b) P1 filled with water; (c) P2 filled with saturated sand; (d) P3 filled with grout; (e) P4 filled with steel fiber grout; (f) steel fiber.

The soil characterization at the test site included direct push sampling to a depth of 15 m and standard penetration tests (SPT) to a depth of 23 m. The soil surrounding the piles is composed of made ground to 3m, with alluvial soil beneath this depth. Saturated sand is the dominant lithology, as shown in Fig. 3a. The groundwater table varies seasonally from 2 to 4 m depth. Ground temperatures from sensors installed in the pile P3 (measured in December/2019) indicate an average value of ~ 23.5 ^{o}C (Fig. 3a). Temperature sensors were installed along the pile length (at the pile center), as shown in Fig. 3b. For the pile filled with water (P1), temperature gradients can induce buoyance-driven natural convection; therefore in this pile temperature sensors were additionally placed closer to the pile edge (Fig. 3b).

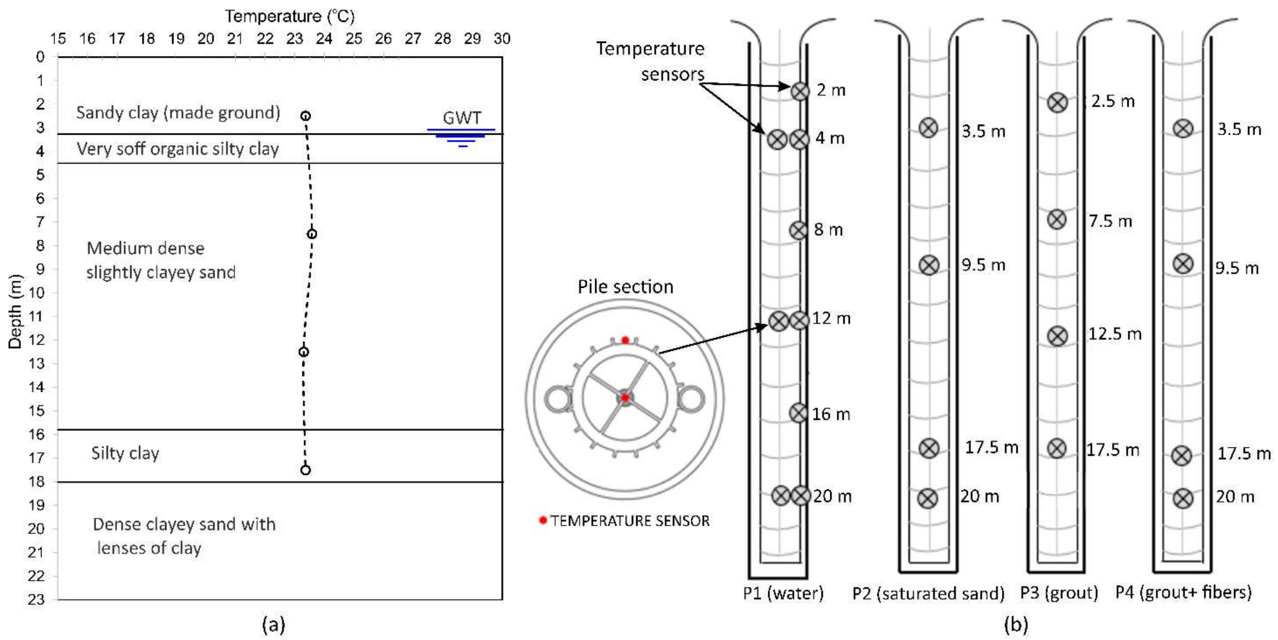

Figure 3. (a) Soil type and undisturbed ground temperature along the depth; (b) depth of the temperature sensors installed into the test piles.

2.2. Thermal response tests (TRT)

Thermal response testing (TRT) is an experimental in situ technique to estimate the ground thermal conductivity and the heat exchanger thermal resistance. Despite the fact that TRT analysis was developed for boreholes, the test is frequently used for energy piles as well. However, it is important to recognize the test limitations, as the time to achieve the steady state is dependent on the pile aspect ratio (AR) and diameter [37].

The TRT is carried out by applying a constant heating power to a circulating fluid in the ground heat exchanger (GHE), and measuring temperature changes at the inlet and outlet of the U-tube. During the heat exchange process, the fluid temperature in the inlet and outlet increases gradually and a heat exchange balance is attained after a long time [38]. For the current work, TRTs were conducted on 4 test piles (Fig. 4a) to determine the thermal conductivity of the soil along the pile length (λ_g) for the design of a ground-source heat pump system at the test site, and to investigate which pile backfill material can provide lower pile thermal resistance. The lower the pile thermal resistance, the higher the energy pile performance [39].

The thermal response test apparatus used in the current study (Fig. 4b) consists of a 0.1 m³ heater hot water reservoir (with 1.5 kW power), a circulation pump, a turbine flowmeter (to measure the water flow rate, and temperature sensors (platinum thermistor sensors, PT-100 class A) within the circulating fluid. The temperature sensors and the flowmeter were connected to a data logger. The characteristics of the equipment and sensors (with absolute errors) used in this study are described in Table 1.

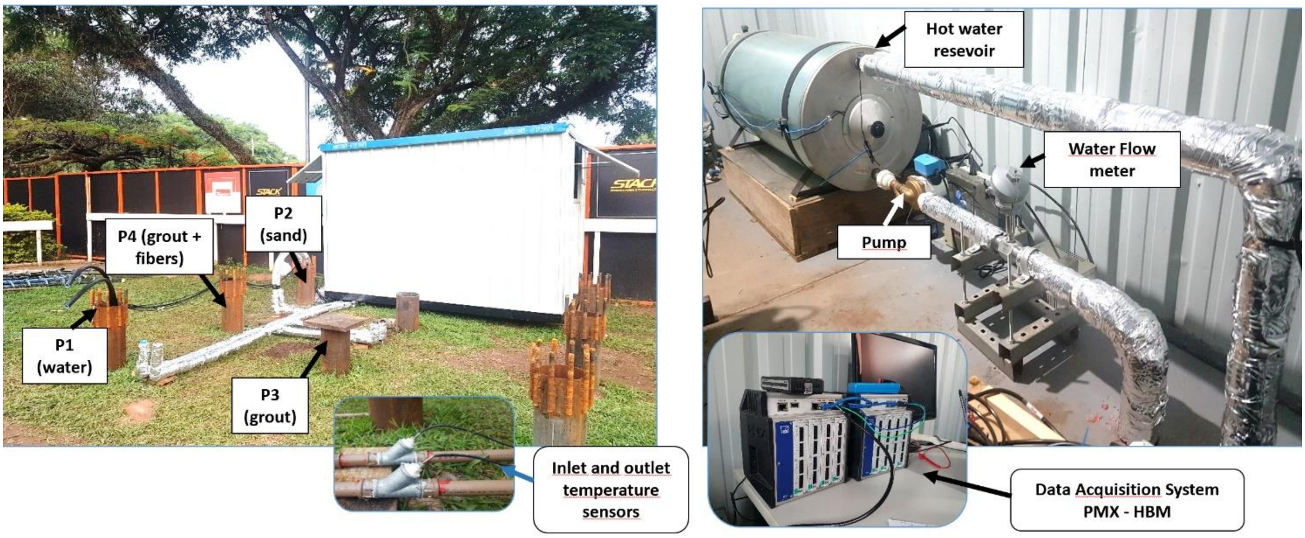

Figure 4. Test piles (a) and TRT apparatus (b).

Table 1- Characteristics of equipment and sensors used in this study.

Equipment / sensor	Characteristics
Circulation pump	TP 40 Thermo G3 circulation water pump, manufactured by Komeco Company
Hot water tank	tank of 0.1 m³ heated by an electrical heater of 1.5 kW power
Data logger	model PMX (Catman®software) manufactured by Hottinger Baldwin Messtechnik Gmbh (HBM)
Flow meter	turbine stainless flowmeter Model SVTL 1”, produced by Contech Indústria e Comércio de Equipamentos Eletrônicos Ltda (absolute error: ±0.5%)
Temperature sensor	PT-100 Class A (absolute error: ±0.15 to 0 °C and ±0.35 to 100 °C, and operation range from 0 to 250 °C), manufactured by Salcas Indústria e Comércio Ltda

Fig. 4a shows the test piles connected to the TRT apparatus installed in a shipping container. The longest distance between a test pile and the container was ~ 3.5 m (Fig. 4a). The pipework was thermally insulated with stone wool, elastomeric thermal pipe insulation, and covered by aluminized foil tape to minimize heat loss and external temperature effects on the results.

For the TRTs, a fixed heat power of 1.5 kW was employed during 72 hours (3 days) with a fluid flow rate of approximately 9 to 10 l/min, and the changes in the fluid inlet and outlet temperatures were recorded over time. For the pile P4 (filled with steel fiber grout), the heating phase duration was 90 hours due to some problem with the inlet temperature acquisition in the beginning of the test. After the end of the heating phase, a recovery test was performed, in which fluid circulation was maintained with no heat input. The duration of the recovery phase varied from 24h to 48h. Table 2 shows the details of the tests.

Table 2- Thermal response tests.

Test	Test pile	Backfill material	Pile length (m)	Test duration (h)	
				Heating	Recovery
TRT 1	P1	Water	23.00	72	-
TRT 2	P2	Saturated sand	22.75	72	48
TRT 3	P3	Grout	23.50	72	48
TRT 4	P4	Steel fiber grout	22.80	90	24

The effective heating power Q (W) applied to the heat carrier fluid during the TRTs was not the nominal value due to external interferences, due to ambient temperature variation and heat losses. As recommended by Banks (2009), the effective heat power values was calculated by Equation 1 using the inlet and outlet temperature difference (in K), the fluid mass flow rate m (in kg/s) and the fluid specific heat capacity C_{pf} (in J/kgK) as follows:

$$Q = mC_{pf}(T_{out} - T_{in}) \quad (1)$$

3. Test interpretation

The results obtained from TRTs enable evaluation of the ground thermal conductivity, λ_g, and the pile thermal resistance, R_b, of the energy piles with different types of backfill material. The λ_g value is often determined by a G-Function where the temperature change as a function of time is determined by solving the diffusion equation for a constant applied heat power q (W/m). The GHE thermal resistance is a steady state parameter, dependent on the pile geometry and thermal conductivity and pipes position. The test results were analyzed in this paper by traditional analytical models and 2D and 3D numerical methods as described below. The best-fit thermal parameters determined by solving the analytical and numerical models were compared with the experimental results, and the root mean square (RMSE) error was calculated for each analysis.

3.1. Analytical models

3.1.1. Infinite line source model (ILSM)

Due to its simplicity, the infinite line source model (ILSM) is the most common 1D analytical model to analyze the thermal response of a vertical ground heat exchanger (GHE). This method is based on the Kelvin's linear heat source, with a constant heat flow (q) [40,41]. By using the ILSM, it is possible to estimate the ground temperature changes (ΔT_g) due to the constant heat power q (W/m) input during the TRT test. The GHE thermal response can be calculated by Equations 2 and 3.

$$\Delta T_g(r_i, t) = \frac{q_t}{4\pi\lambda_g} \int_{\frac{ri^2}{4\alpha_g t}}^{\infty} \frac{e^{-u}}{u} du = \frac{q_t}{4\pi\lambda_g} E_i\left(\frac{{r_i}^2}{4\alpha_g t}\right) = \quad (2)$$

$$\Delta T_g \cong \frac{q}{4\alpha\lambda_g}\left[\ln\left(\frac{4\alpha_g t}{r^2}\right) - \gamma\right] \quad (3)$$

Where q_t is the constant heat injection rate, λ_g and α_g are the ground thermal conductivity (W/mK) and diffusivity (m²/s) respectively, r is the radial coordinate, and Y is the Euler's constant

(0.5772). The simplification of the Equation 2 to a log-linear relationship is shown in Equation 3, when the early portion of data is neglected. The first results of the test are ignored because the initial response is influenced by the thermal properties of the borehole [42]. In common practice, the neglected initial period *t* corresponds to a Fourier number (or normalized time) *Fo* = 5 [43].

$$F_0 = \frac{\alpha_g t}{{r_b}^2} \tag{4}$$

Where α_g is the ground thermal diffusivity ($\alpha_g = \frac{\lambda_g}{\rho C_{pg}}$, where ρC_{pg} is the volumetric heat capacity of the ground), r_b is the is the borehole (or pile) radius, and *t* is the time after the beginning of the heating process. To determine the test duration *t* corresponding to *Fo* = 5, the α_g value estimated in this study was 8.14 x 10^{-7} m²/s, resulting in a neglected time *t* equal to 25 hours (Equation 4). The heat transfer steady state assumption allows for a constant pile thermal resistance and the ground thermal conductivity can be determined by the Equation 5.

$$\lambda_g = \frac{Q}{4\pi m H} \tag{5}$$

Where the *m* is the slope of the linear relationship between mean fluid temperature with the logarithm of time, *Q* is the heat injection rate, and *H* is the GHE length. The pile thermal resistance R_b can be estimated from the intercept in *ln*-space, by the Equation 6.

$$R_b = \frac{1}{4\pi\lambda_g}\left[\frac{T(t_{1hr}) - T_0}{m} - ln\left(\frac{4\alpha_g t_{1hr}}{\gamma {r_b}^2}\right)\right] \tag{6}$$

The exponential integral version of line source model (Equation 2) has also been used in this study to determine the values of λ_g and R_b. For this case, a code was developed to calculate the full analytical solution.

The temperature data obtained during the recovery phase of test can equally be used to determine the ground thermal conductivity [44]. In this case, the gradient of the graph of fluid temperature against ln(*t*/*t'*) was built, as described in Equation 7, where *t'* is the initial time of the recovery phase.

$$\Delta T_f \cong \frac{q}{4\pi\lambda}\left\{\ln\left(\frac{t}{t'}\right)\right\} \tag{7}$$

3.1.2. Solid Cylindrical Source Model (SCSM)

According to Loveridge and Powrie [6], the temperature response of most of pile heat exchangers will be somewhere between the Line Source Model and the Solid Cylinder Source Model (SCSM) proposed by Man et al. [45].

The SCSM is an improvement on the classic infinite cylindrical source model, a 1D analytical method to simulate the heat transfer of GHE [40, 46]. This model takes into account the size of the GHE, and the heat flux is directly applied from the cylindrical surface. In this approach, the cylindrical heat source is "hollow" and the heat is considered to flow outwards.

Modified from the classical model, a new solid cylindrical source model was recently proposed, in which the cylindrical cavity is filled with the same homogeneous medium of the hole domain, called "solid" cylindrical heat source model, SCSM [45]. In this model, the ground is regarded as a homogeneous infinite medium with a uniform initial temperature; however, it assumes that the heat can flow inwards from the heat source surface into the pile backfilling, as well as outwards to the ground.

In the current work, the SCSM was used to analyse the TRT results. Equation 8 shows the expression to estimate the temperature rise at the heat source (Θ_c) for $R = 1$ (R = pile radius). Equation 9 illustrates the normalised form considering the normalised temperature (φ) and the Fourier number (F_0), for a constant of heat injection rate q (W/m).

$$\Theta_c = \frac{q}{\lambda_g}.G(Fo) \quad (8)$$

$$\Phi = G(Fo) \quad (9)$$

Man et al. [45] proposed a simplified empirical expression shown in Equation 10 for the normalized temperature (Φ):

$$\ln(\Phi) = -2.321016 + 0.499615.[\ln(F_0)] - 0.027243.[ln(F_0)]^2 - 0.00525.[\ln(F_0)]^3 + 0.000264311\,[ln(F_0)]^4 + 0.00006873912[\ln(F_0)]^5 \quad (10)$$

To determine the pile thermal resistance R_b, the initial test time ($F_0 < 5$) was neglected and the steady state condition was assumed. Therefore, the pile thermal resistance was considered constant and was calculated using the Equation 11, where ΔT_f is the fluid temperature variation.

$$\Delta T_f = q.R_b + \frac{q}{\lambda_g}.G(Fo) \quad (11)$$

In this study, the Microsoft excel solver tool was used to simultaneously estimate the ground thermal conductivity and the pile thermal resistance values. The RMSE difference between computed and fluid temperature observed values variation were minimised.

3.1.3. Semi-empirical pile G- Function

The semi-empirical pile G-Function, proposed by Loveridge and Powrie [6] was also used to evaluate the tests results. This analytical solution is an update of Eskilson's work [43], and takes into account the typical energy piles geometries and the transient heat storage within the pile. This is achieved by using separated G-functions, one for the ground temperature responses and other for the concrete, G_g and G_c respectively. Three elements must be considered, as shown in Equation 12.

$$\Delta T_f = qR_p + qR_cG_c + \frac{q}{2\pi\lambda_g}G_g \quad (12)$$

Where q is the constant heat flux (W/m), R_p is the resistance of the pipes including the fluid, G_c is the concrete G- function, G_g is the transient response of the soil around the pile, and R_c is the concrete thermal resistance (for the current case is the combination of steel pipe pile and the infill material resistances). The pipe resistance can be defined as the sum of the pipe convective resistance associated with the flowing fluid and the pipe conductive resistance associated with pipe material as follow:

$$R_p = R_{pcond} + R_{pconvec} \quad (13)$$

The pipe convective resistance $R_{p\,convec}$ is usually calculated using the following expression:

$$R_{p\,conv} = \frac{1}{2n\pi r_i h_i} \quad (14)$$

Where n is the number of pipes within the pile, r_i is the pipe internal radius and h_i is the convective heat transfer coefficient, which can be calculated by the Dittus-Boelter equation [6]. The pipe conductive thermal resistance $R_{p\,cond}$ can be estimated by Equation 15, where r_o is the pipe outer radius.

$$R_{p\,cond} = \frac{\ln(r_o/r_i)}{2n\pi\lambda_p} \quad (15)$$

To estimate the pile thermal resistance with the G-Function model it was needed to sum the concrete thermal resistance (R_c) and the pipe thermal resistance (R_p). The empirical G-functions were developed by numerical derivations, considering constant surface temperature, typical pile aspect ratios, different pipes arrangements and pile diameters from 300 to 1200 mm. The G-Functions for G_g and G_c are presented in Equations 16 and 17. The curve fitting coefficients are provided in Loveridge and Powrie [6] for different aspect ratios.

$$G_g = a[\ln(F_o)]^7 + b[\ln(F_o)]^6 + c[\ln(F_o)]^5 + d[\ln(F_o)]^4 + e[\ln(F_o)]^3 + f[ln(F_o)]^2 + g[\ln(F_o)]h \quad (16)$$

$$G_c = a[\ln(F_o)]^6 + b[\ln(F_o)]^5 + c[\ln(F_o)]^4 + d[\ln(F_o)]^3 + e[\ln(F_o)]^2 + fln(F_o) + g \quad (17)$$

The solver tool from Microsoft excel was used to estimate the values of λ_g and R_c based on the minimum RMSE fit from the experimental data, considering all test data. The results presented in this study, obtained by Equation 12, represent the lower bound G-functions for both G_g and G_c, considering an aspect ratio (AR) of 50 and the pipes near the pile edge. This combination provides the best fit thermal parameters when compared with the experimental data.

3.2.Numerical models

For this study, 2D and 3D numerical models were developed to determine the ground and pile thermal parameters. Both models have been set up using the finite element software COMSOL Multiphysics (Version 5.4). The 2D models were developed to investigate the thermal behavior of the conductive filling materials: sand, grout and steel fiber grout. Because of the occurrence of natural convection during the TRT on the pile filled with water (pile P1), a 3D numerical model was established for this pile case.

A parametric analysis was made to find the best pairs of ground thermal conductivity (λ_g) and the thermal conductivity of the backfill material (λ_c) values, which is related to the pile thermal resistance. More than one combination of values can provide best-fit thermal conductivity and thermal resistance from experimental results in terms of minimum RMSE [47, 48]. However, as there are a good number of tests, it was possible to compare the results and check the validity of the values. More details of each numerical models are described in the following sections.

3.2.1. 2D numerical simulation

A two-dimensional model was developed to investigate the heat transfer during the TRT tests conducted on piles P2, P3 and P4. The simplification for a two dimensional analysis is justified by the short test duration (72 hours). The model utilized the transient heat transfer in solids module in COMSOL Multiphysics which solves the Fourier diffusion (Equation 18):

$$\rho c_p = \frac{\partial T}{\partial t} = \nabla(\lambda \nabla T) \qquad (18)$$

Where ρC_p (J/m³/K) is the volumetric heat capacity, T (K) the temperature, t (s) the time, λ is the effective thermal conductivity (W/m/K). The domains considered were the soil, assumed to be homogeneous, the steel pipe pile, and the pile backfill material. The HDPE pipe and the heat carried fluid (water) were not modelled. This numerical approach allowed to determine the thermal pile resistance, which is a combination of the pile backfill material and steel pipe pile resistances.

The 2D model was developed for the hollow pile cross-section as illustrated in Fig. 5. To solve the aforementioned heat diffusion equation, appropriated boundary conditions needed to be provided. The heat carried fluid was simulated using the heat flux calculated from the TRT (W/m) by Equation 1. This flux was applied as a power per unit area, distributed around the pipe circumference (Equation

19). The heat flux fluctuation during the tests were considered in the model with variation every 10 seconds.

$$q = \frac{Q}{n\pi L d_o} \quad (19)$$

Where Q is the heat power (W), n is the number of pipes, L is the pipe length (m) and d_o is the outer pipe diameter (m).

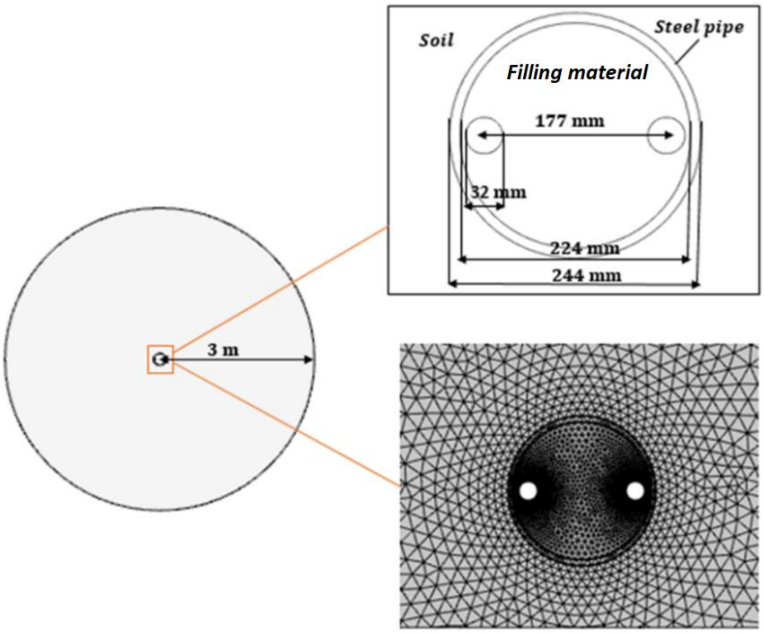

Figure 5. Energy pile section for the 2D numerical model.

The contact boundary between the backfilling material, steel pipe pile and the soil were assumed to meet the continuity condition. The initial ground and pile temperatures were set to be equal to the undisturbed ground temperature measured before the experimental tests (Table 4). A zero heat flux boundary condition (thermal insulation) was applied at the edges of the ground domain. Practically no changes in the boundary temperature were observed for a soil domain of 3 meters radius, confirming that the location of the boundaries did not impact the outcome of the simulation.

The domains were meshed using triangular elements with a maximum size of 13 mm at the pile boundary and minimum size of 2 mm at the pipe boundary, used in past experience [6]. A mesh sensitivity analysis was conducted, and it was adopted a final mesh with 61,114 elements after verifying that more elements (in different arrangements) were not beneficial. By increasing the mesh from 60,000 elements to 140,000 resulted in only a 0.002°C reduction in RMSE, indicating that the results presented in this study are mesh independent. In this case, each numerical simulation took approximately 12 h on a high-performance desktop computer with 3.4 GHz processors and 32 GB of RAM.

The 2D cross-section model was validated with the TRT datasets and the analysis were done for the same duration as the experimental tests. To achieve the best fit data, a parametric analysis was made to find a combination of λ_g, λ_c, C_{pg}, and C_{pc} values (thermal conductivities and specific heat capacities of the ground and backfill material, respectively) that best fit the experimental data with the minimum RMSE. Initial input parameters were obtained from the current analytical model results (ILSM, SCSM) and from the literature [49, 50, 51, 52]. The thermal conductivity of backfill material used as an input value was firstly calculated by the multipole model [53] considering the pile thermal resistance obtained from ILSM model.

The multipole model [54] is a complex algorithm to estimate the thermal resistance for any configuration of pipes in a borehole. The model assumes that each pipe is a line heat source or a multipole to solve the steady state heat transfer problem by superposition to determine the heat flux of each pipe [55]. The multipole model is regarded as an accurate method to calculate the thermal resistance or circular cross section ground heat exchangers when compared with numerical analysis, as shown by Lamarche et al. [56], Liao et al. [57] and Go et al [58].

The resistance for first-order multipoles can be calculated by Equation 20, which is a relatively simple expression and it can be applied for the case of two pipes systems [53].

$$R_b = \frac{1}{4\pi\lambda_c}\left[ln\left(\frac{r_b}{r_o}\right) + ln\left(\frac{r_b}{s}\right) + \sigma ln\left[\frac{{r_b}^4}{{r_b}^4 - \left(\frac{s}{2}\right)^4}\right]\right] + \frac{1}{2}R_p \qquad (20)$$

Where, $\sigma = \frac{\lambda_c - \lambda_g}{\lambda_c + \lambda_g}$ and $\frac{1}{2}R_p = R_{p\,convc} + R_{p\,cond}$.

In Equation 20, R_b is the borehole thermal resistance, λ_c is the thermal conductivity of backfill material, r_b and r_o are respectively the borehole radius and pipe outer radius, and s is the space between the pipes. The R_{pconv} and R_{pcond} can be determined by Equations 14 and 15.

For the 2D numerical models, more than 50 interactions were required to find the best fit solutions with a computation time of 7 hours for each interaction, using a desktop computer with 4.9 GHz processor and 32 GB RAM. To estimate the pile thermal resistance, the temperature variation at the pile boundary was analyzed for the best fit parameters. The R_b value was determined by Equation 21, where ΔT is the difference between fluid and pile wall temperatures at the steady state phase.

$$\Delta_T = qR_b \tag{21}$$

3.2.2. 3D numerical simulation

For the pile filled with water (P1), the ground thermal conductivity and the pile thermal resistance estimations are affected by buoyancy effects. Analytical methods such as the ILSM, SCSM and pile G-Functions are not appropriated for this case, resulting in higher values for the soil thermal conductivity. Previous studies suggested that natural convection increases the heat transfer rate in the annulus region and consequently reduces the effective thermal resistance of the borehole [55, 59, 60, 61]. Additionally, field measurements demonstrated that the groundwater filled borehole resistance is affected by the heat transfer rate and the temperature in annulus region [59, 60].

Although several investigations revealed the correlation between the natural convection in water filled boreholes and its thermal resistance, there is a lack of information about design procedures and modelling approaches. To simulate free convection effect, a three-dimensional model was developed in COMSOL Multiphysics. All the domains were considered in the 3D model: the soil, the steel pipe pile, the water as filling material, the HPDE pipes embedded in the piles, and the heat carried fluid (water).

In this model, conductive heat transfers within the ground and the pipes were simulated as well as conductive-convective heat transfer within the filling material and carrier fluid. Two modules in COMSOL package were used: heat transfer in solids and fluid flow. Conduction heat transfer in the transient regime is calculated by Fourier equation (Equation 18). The combined heat transfer by conduction and convection in the model occurs in the heat conducting fluid that circulates through the HDPE pipes and is calculated by Equation 22.

$$\rho_m C_{p,m} \frac{\partial T}{\partial t} + \rho_m C_{p,m} u \nabla T = \nabla(k_m \nabla T) + Q \quad (22)$$

In Equation 22, ρ_m is the water density in kg/m³, u is the fluid velocity in m/s, k_m is the thermal conductivity of the medium in W/mK, $C_{p,m}$ is the specific heat of the medium in J/ KgK, and Q is the heat source in W/m³. .

Fluid flow in the pipes is assumed to be turbulent and that this process is reduced to a 1D representation by a cross section average velocity and pressure. To determine this, the heat transfer in pipes module was used. This simplification avoids more refined meshes to simulate the pipes cross section [62]. The coupling to the 3D heat transfer model was done through the temperature calculated on the pipe wall [63]. The equations used for the calculation of heat transfer and temperature in the pipes are respectively Equations 23 and 24.

$$\rho_w A C_{p,w} \frac{\partial T}{\partial t} + \rho_w A C_{p,w} u \nabla T = \nabla(k_m \nabla T) + f_D \frac{\rho_w A}{2 d_n} |v| v^2 + Q_v + Q_{wall} \quad (23)$$

Q_{wall} corresponds to the heat transferred by the tube wall, and can be estimated by the equation below.

$$Q_{wall} = \frac{2\pi}{\frac{1}{r_i}\left[N_u\left(\frac{k_p}{d_h}\right)\right] + \frac{\ln(r_o/r_i)}{k_p}} (T_{w2} - T) \quad (24)$$

In the equation r_o and r_i are respectively the external diameter and internal diameter of the HDPE pipe, in m, k_p is the thermal conductivity of the pipe in W/mK, T_{w2} is the temperature outside the pipe and N_u is the Nusselt number that depends on flow regime, in this case turbulent. All the equations presented were solved by the finite element method implemented in the COMSOL Multiphysics program.

A fluid flow rate of 10.22 l/min was specified as boundary condition in the inlet pipe. This simplification is justified by the considerable slenderness of the pipe. The flow in the pipe was simulated by Churchill's friction model [64] which computes the internal convection effect. A reference atmospheric pressure was set in the outlet pipe for the purpose of forced convection.

To simulate the effect of the natural convection of the water used as backfilling material, firstly, the water domain was regarded as laminar flow and convection was simulated by equation 22. The following flow boundary conditions were set in the model: i) gravity was applied to the surface of the fluid so that there is natural convection; ii) the fluid was considered to be poorly compressible so that the density of the water varied as a function of temperature; iii) the pressure was set to be zero on the liquid surface.

The soil domain dimensions have been defined after sensitive analysis of the temperature effect on the boundaries. The geometry and extent of geothermal energy pile considered in the present analysis is shown in Figure 6.

To solve the system equations, appropriate boundary conditions need to be provided: i) zero water velocity applied to the HDPE pipe walls, which means that the fluid in the pipe wall is not moving; ii) a reference atmospheric pressure was defined at the outlet pipe so that the effect of forced convection is considered; iii) thermal insulation of the ground domain and the two surfaces at the top and bottom of the model. In this condition, the effect of thermal recharge due to solar irradiation on the soil surface was neglected.

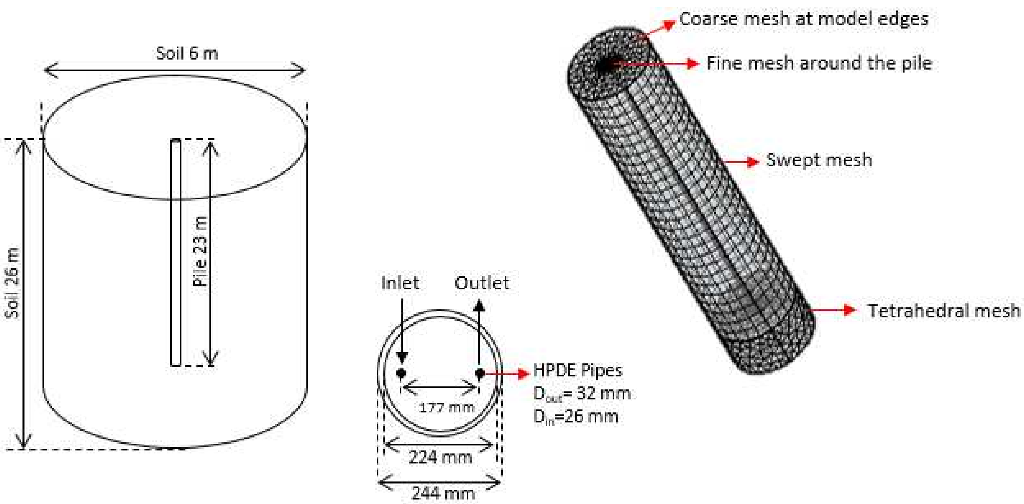

Figure 6. 3D numerical geometry model.

Due to the high aspect ratio, swept meshing was applied to the pile length to provide efficient and accurate results with less elements. For the 3 m of soil below the pile tip, a coarse free tetrahedral mesh was set up. A mesh refinement analysis was made seeking an optimum accuracy and reasonable computational effort and showed that an increase to 150,000 elements resulted in only 0.006°C reduction in RMSE. The final mesh adopted contains 21,851 elements, with a greater mesh refinement within pipes and pile region, where the temperature gradient was higher and where free convection occurred. In this case, each numerical simulation took approximately 36 h on a high-performance desktop computer with 3.4 GHz processors and 32 GB of RAM.

The material parameters used as input values in the model are listed in Table 3. The value of ground thermal conductivity was determined by the analytical methods applied to the experimental results. The other thermal parameters were taken from the literature.

Table 3. Material properties.

Material	Thermal Conductivity (W/mK)	Specific Heat (J/KgK)	Density (kg/m^3)	Source
Soil	2.6	1597	2000*	Analytical methods/ *[65]
Steel Pile	54	465	7833	[49]
Water	0.6	4186	1000	[52]
HDPE Pipe	0.385	-	-	[66]

The initial temperature for all the domains (ground, pile, water and pipes) were set to be 23.8°C (average ground temperature at the test site). The time dependent carried fluid temperature change was set at the inlet point T_{in} (t) provided by the experimental TRT data. The outlet temperature T_{out} (t) was accessed from the numerical analysis by the Integration Nonlocal Coupling selected on the outlet point in the geometry. The temperature changes were also analyzed at the same positions of the temperature sensors installed into the pile along the central vertical axis and at the edge.

The pile and pipes average temperatures were numerically determined via surface integration. During the test, at steady state stage, the pile and pipes temperatures become constant with time. Similarly to the 2D numerical model, the pile thermal resistance was calculated by Equation 21 using the constant heat power obtained from the experimental data.

4. Results

4.1. In-situ TRT tests

The results of the 4 TRTs carried out in this study are presented in Fig.7. The actual applied power variation was calculated by Equation 1. The ground initial temperatures (measured inside the piles), the effective heating power, the water flow rate, and the difference between the inlet and outlet fluid temperatures (T_{in} - T_{out}) at the end of the heating phase are detailed in Table 4. The heat rate supplied to the heat ground exchanger was 1.5 ±0.25 kW. The difference between the inlet and outlet fluid temperatures was approximately 2 °C at the end of the heating phase of the tests.

Table 4. Average initial ground temperature along the pile and effective heat power applied to tests.

Test	Pile filling material	Heat Power input (W/m)	Ground initial temperature (°C)	T_{in} -T_{out}, (°C)	Water flow rate (l/min)
TRT-1	water	60.4	23.8	1.97	10.03
TRT-2	saturated sand	58.2	24.3	2.18	10.51
TRT-3	grout	59.8	23.8	2.00	9.83
TRT- 4	grout + fibers	63.0	24.1	2.01	9.35

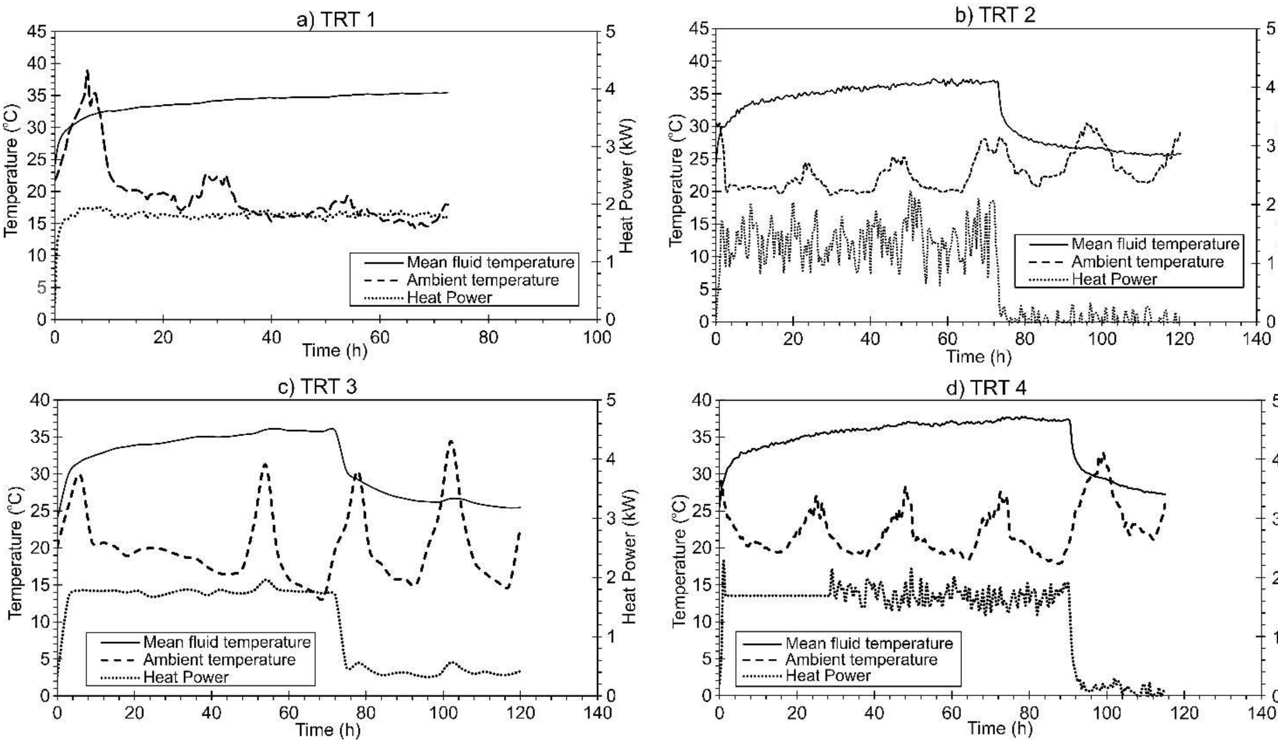

Figure 7. Thermal response tests results.

Fig. 8 compares the fluid temperature temperature variation during the tests, with Fig.8a showing absolute temperature measurements and Fig. 8b showing a comparison in terms of non-dimensional temperature ($\Phi_f = 2\pi\lambda_g \Delta T_f / q$) and non-dimensional time ($F_o = \alpha_g \, t / r_b^2$).

The slope of the curves shown in Figure 8 is controlled mainly by the ground thermal properties, which is the same for all piles. However, some differences are also caused by the different pile filling material thermal properties. The initial part of the curves are similar for all tested cases, and after approximately 60 minutes, the increase rate of Φ_f is reduced for the pile P4, probably due to the higher thermal conductivity of the steel fiber grout (lower thermal resistance) compared to the other filling materials. Additionally, the rate of increase gradually decreases for the pile filled with water, possibly due to the buoyancy effect, which enhances the heat flux between the pile and surrounding soil, reducing R_b. The results for the piles filled with saturated sand and grout are almost identical, indicating similar thermal performance.

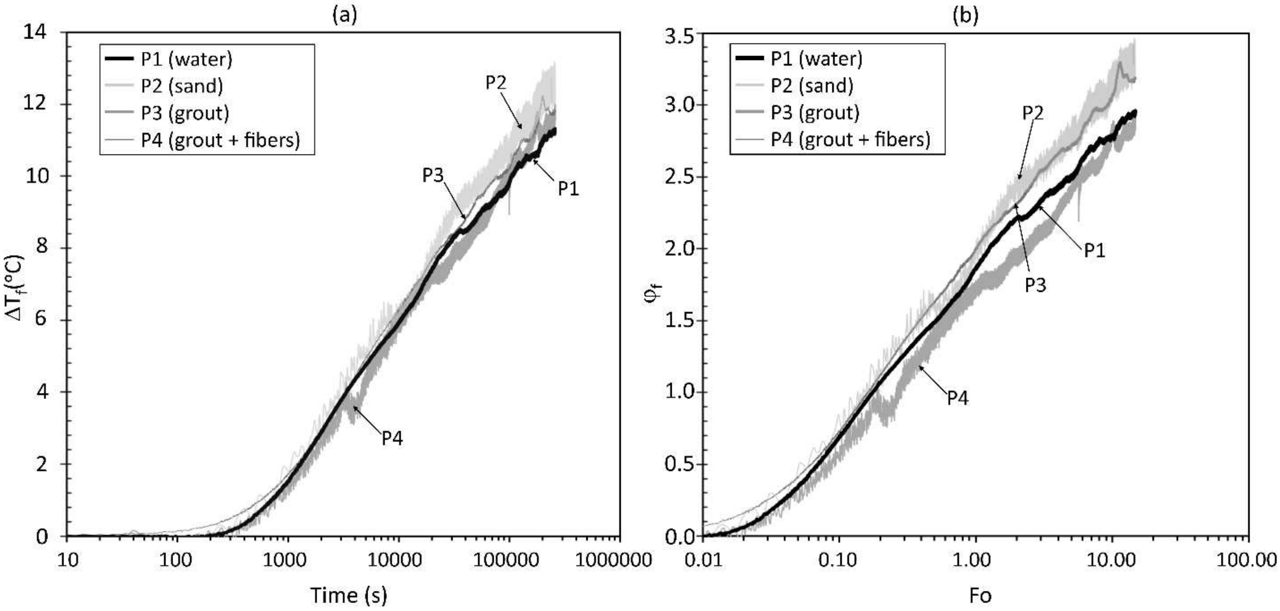

Figure 8. (a) Fluid temperature and (b) normalized fluid temperature variation during the TRTs.

Figure 9 shows the temperature variation inside the piles during the heating phase of the TRTs. The pile temperatures tended to be higher at the clay layers for piles P2, P3 and P4 (grout and sand fillings), due to the lower ground thermal conductivity of the clayey layer (Figs. 9c-e). Additionally, during heat injection, the average fluid temperature decreases with depth [15] and therefore greater temperature change is observed at the top of the pile than at the base (Figs. 9c-e). On the other hand, the pile filled with water (P1) showed a different behaviour (Fig. 9a,b), indicating higher temperatures in the middle height of the pile (~12 m depth). The mechanism of water convection, discussed later in the paper, increases the temperature in the middle of the pile.

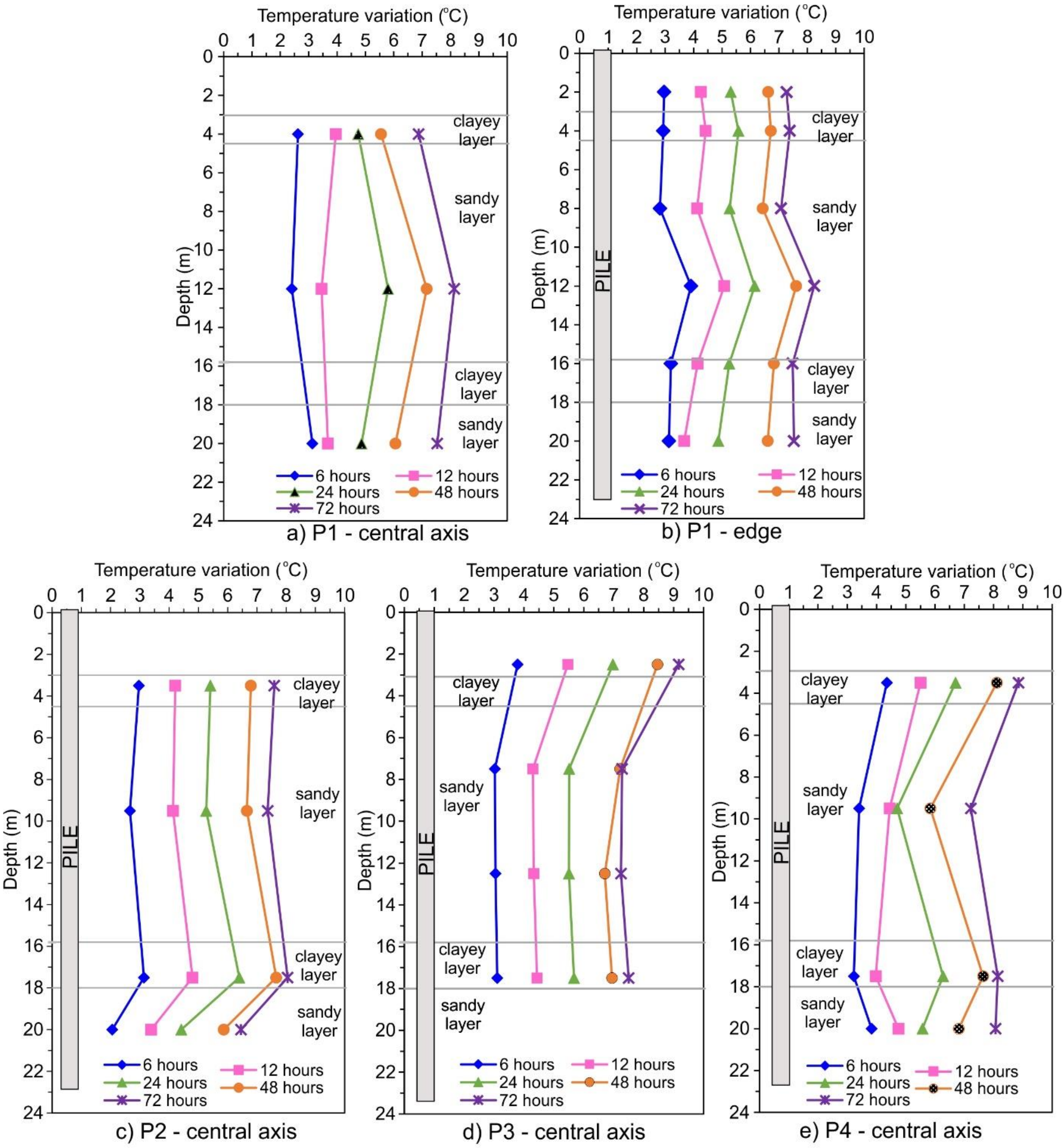

Figure 9. Pile temperature profile at different times: a,b) P1; c) P2, d) P3, e) P4.

4.2. Results of the analytical models

Figs. 10 to 13 compare the analytical model results with the measured data from the TRT tests. These figures also include the RMSE values for the parameters estimated for F_o >5.

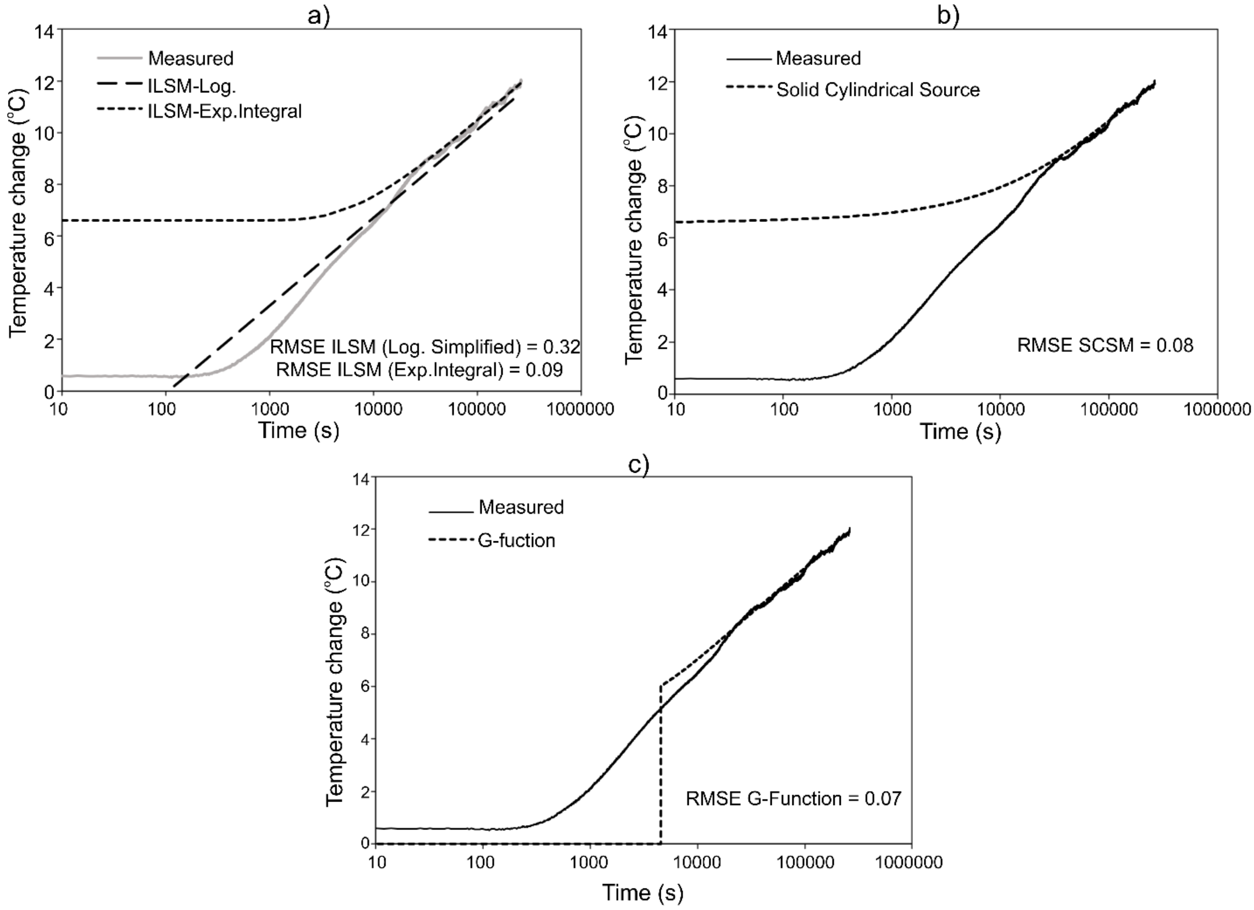

Figure 10. Analytical models vs. measured data from TRT-1 (pile filled with water).

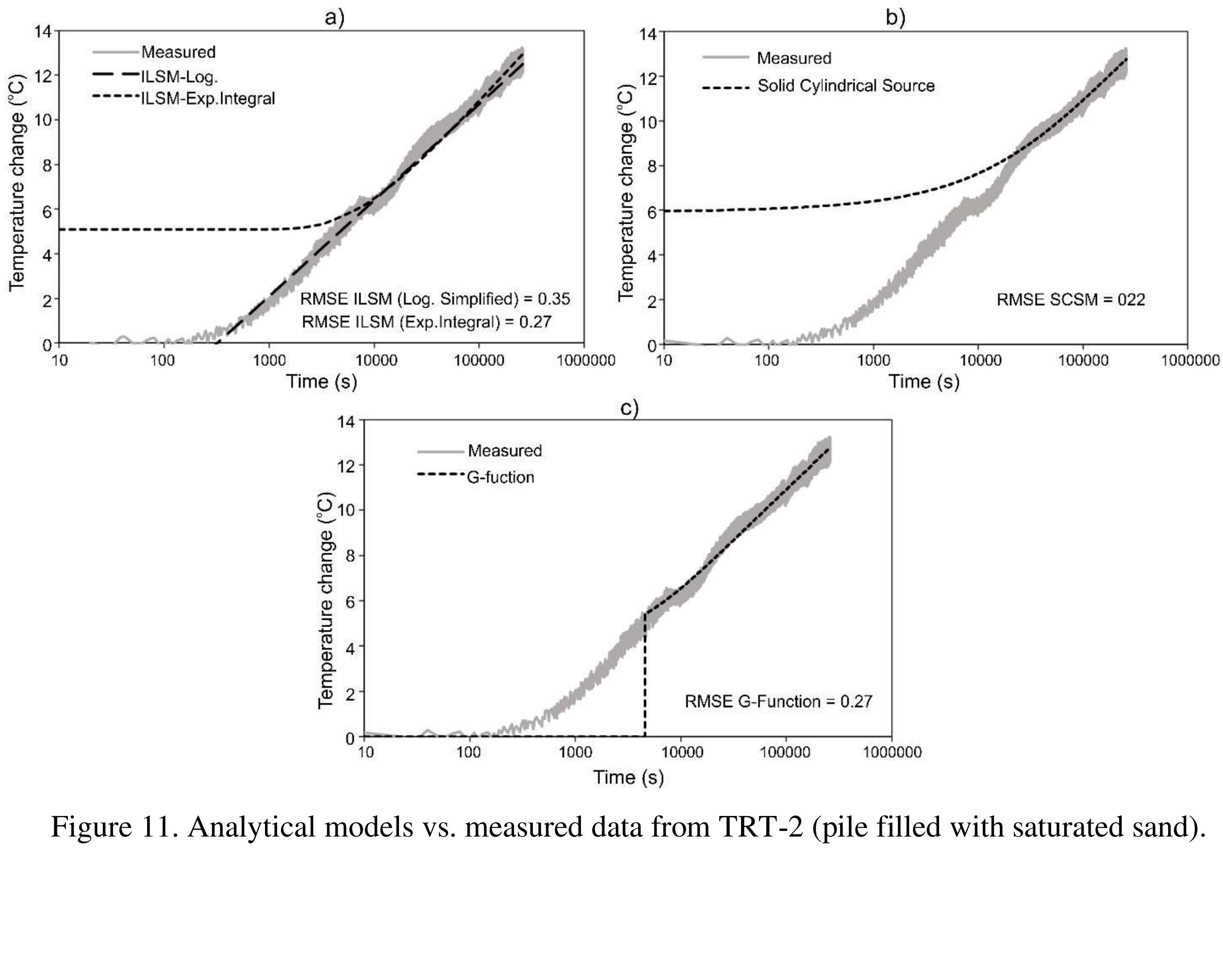

Figure 11. Analytical models vs. measured data from TRT-2 (pile filled with saturated sand).

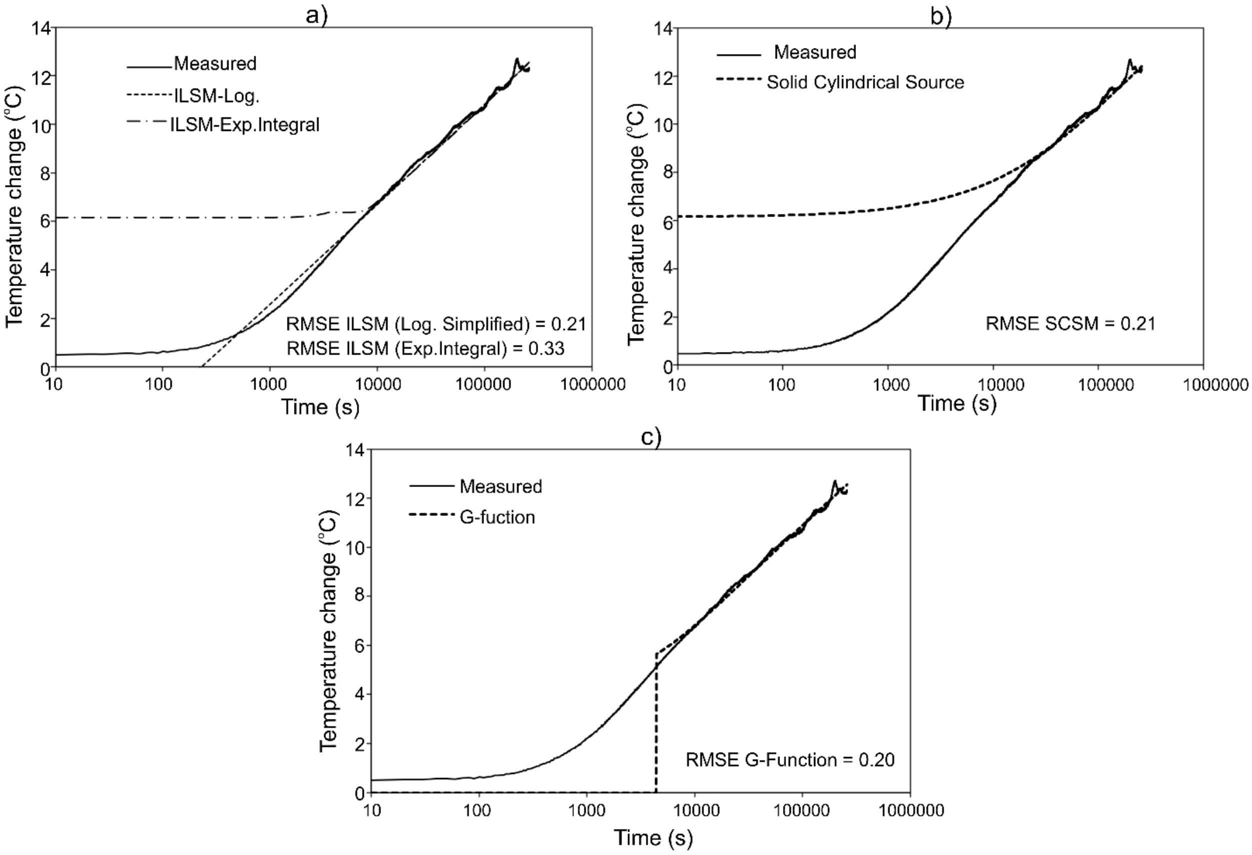

Figure 12. Analytical models vs. measured data from TRT-3 (pile filled with grout).

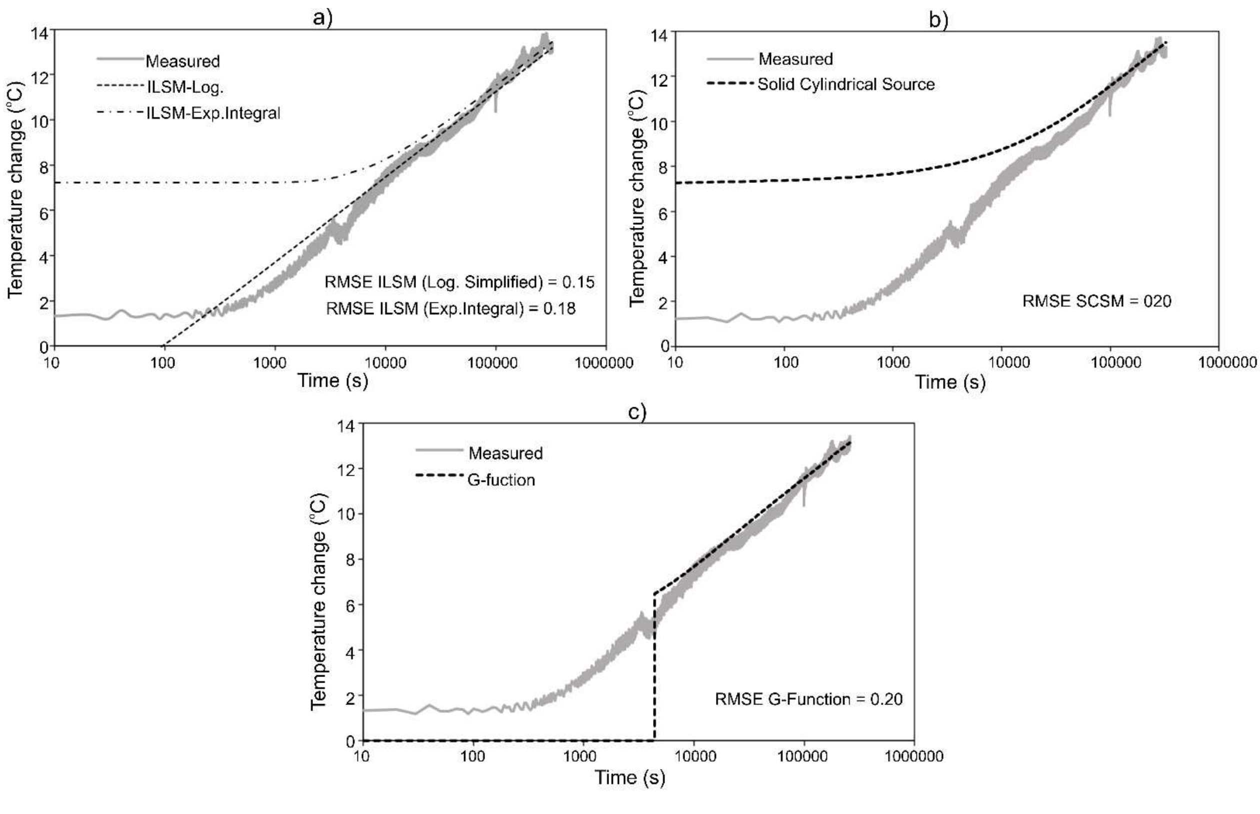

Figure 13. Analytical models vs. measured data from TRT- 4 (pile filled steel fiber grout).

For the ILSM, three different procedures were used to calculate the ground thermal conductivity: (*i*) determination of gradient *m* from regression of temperature change with the logarithm of time (ILSM-Log. Simplified), (*ii*) the full version of the analytical solution (ILSM-Exp. Integral); and (*iii*) the gradient *m* calculated using the test results of the recovery phase (ILSM-Recovery).

Table 5 summarized the results of pile thermal resistance (R_b) and ground thermal conductivity (λ_g) estimated by the analytical approaches. The analytical models showed good agreement with experimental data, and achieved similar accuracy evaluated according to the root mean square error (RMSE). Based on the results obtained for the tests on piles P2 and P3 shown in Table 5, the average ground thermal conductivity along the pile length can be assumed as ~ 2.60 W/mK.

Table 5. Resulst of ground thermal conductivity and pile thermal resistance from analytical models.

TRT	Analytical method	λ_g(W/mK)	R_b (mK/W)	RMSE
TRT – 1 (pile with water)	ILSM - Log Simplified	3.36	0.102	0.32
	ILSM – Exp. Integral	3.26	0.105	0.09
	SCSM	3.35	0.105	0.08
	G-Function	3.14	0.107	0.08
	Average values	3.28	0.105	0.14
TRT – 2 (pile with saturated sand)	ILSM - Log Simplified	2.64	0.096	0.35
	ILSM – Exp. Integral	2.51	0.094	0.31
	ILSM -Recovery Phase[1]	2.60	-	0.36
	SCSM	2.58	0.095	0.22
	G-Function	2.72	0.101	0.27
	Average values	2.61	0.097	0.30
TRT – 3 (pile with grout)	ILSM - Log Simplified	2.71	0.103	0.21
	ILSM – Exp. Integral	2.63	0.101	0.33
	ILSM -Recovery Phase[1]	2.36	-	0.28
	SCSM	2.70	0.099	0.21
	G-Function	2.67	0.108	0.20
	Average values	2.61	0.103	0.25
TRT – 4 (pile with grout + fibers)	ILSM - Log Simplified	3.25	0.106	0.15
	ILSM – Exp. Integral	3.17	0.108	0.22
	ILSM -Recovery Phase[1]	2.39	-	0.40
	SCSM	3.24	0.108	0.20
	G-Function	3.20	0.114	0.20
	Average values	3.05	0.109	0.23

[1] *Start time after 5 hours*

In analytical models the convection effects that occurred in the water was not taken into account for TRT-1. Consequently, the results of the analysis showed higher values of ground thermal conductivity (Table 5), as the heat flux between the pile and surrounding soil increased. The average soil thermal conductivity found by analytical analysis for the TRT-1 was ~ 3.3 W/mK, which combined the effects of conduction and convection heat transfer in the backfill material. This value is 26% higher than the ground thermal conductivity found in TRT-2 and TRT-3 (of 2.6 W/mK), reflecting the contribution of the convection effects for the pile filled with water to the heat transfer mechanism.

The average value of λ_g obtained from TRT-4 (pile filled with steel fiber grout) was ~ 3.0 W/mK. However, the value of λ_g obtained from the recovery phase was ~ 2.4 W/mK. The recovery method allows the determination of ground conductivity independent of pile resistance and hence is most reliable. Therefore, the assumed value of 2.60 W/mK is considered reasonable for the soil surrounding the test piles. The results detailed in Table 4 indicate that the ILSM (using data of heating or recovery phases) has advantages compared to the other models, because it is simple to use and gives similar results compared to the other models.

4.3. Numerical analysis

4.3.1. 2D Numerical model (for piles P2, P3, and P4)

In this study, parametric analyses were carried out varying the ground thermal conductivity and thermal conductivity of the pile filling material. More than 50 interactions were needed to find the best-fit parameters for each test. Fig.14 illustrates the contour plots of the parametric analyses conducted for TRT-2, TRT-3 and TRT-4, and shows the relationship between the thermal conductivity values which is correlated with the pile thermal resistance. The results of the parametric analyses are shown on Table 6 for the minimum RMSE values.

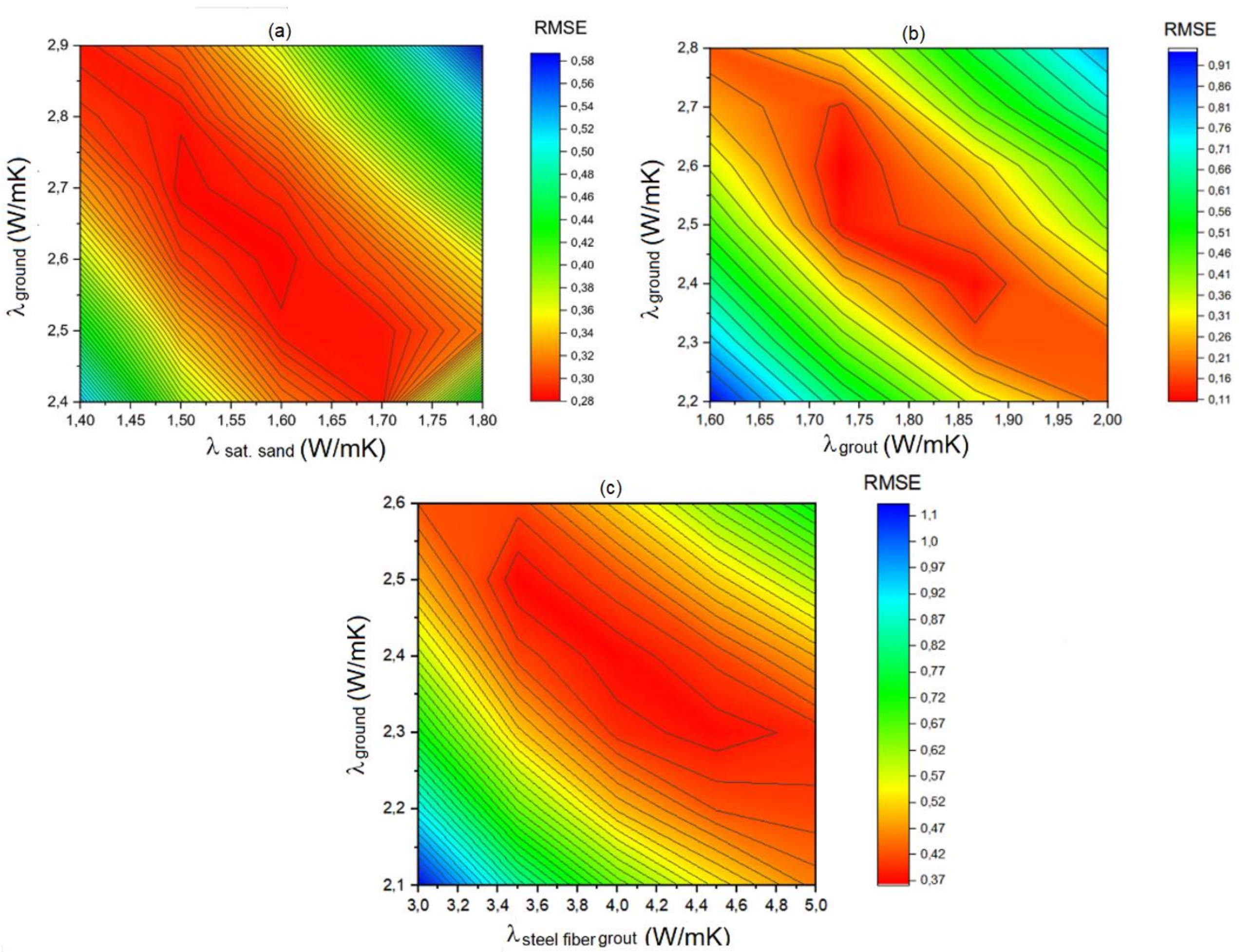

Figure 14. Results of two-parameter-fitting method and root mean square error (RMSE), after Wagner et al. (2012), of the 2D numerical analysis performed for: (a) TRT-2; (b) TRT-3; and (c)TRT-4.

Table 6. Values of ground thermal conductivity and pile thermal resistance from 2D numerical analysis.

Test	Filling material	Filling material properties: Thermal Conductivity (W/m.K)	Density (kg/m³)	Specific heat Capacity (J/kg.K)	Ground: λ_g (W/mK)	Pile: R_b (mK/W)	RMSE
TRT-2	Sand	1.60	1800[1]	1380[1]	2.6	0.093	0.28
TRT-3	Grout	1.75	2000[2]	990[2]	2.6	0.086	0.11
TRT-4	Grout + fibers	4.00	2000[3]	990[3]	2.4	0.061	0.36

[1] [22]; [2] [23]; [3] assumed to be equal for grout with a and without fibers.

From the parametric analysis, the thermal conductivity of the pile filling material was 1.60 W/mK for grout, and 1.75 W/mK for saturated sand, which justifies the similar values of piles thermal resistances. The thermal conductivity found for the steel fiber grout was considerably higher and consequently a lower value of pile resistance was obtained.

Claesson and Hellström, [38] observed that the thermal resistance increases with the distance between the pipes and the borehole wall, and that the thermal resistance of the filling material is inversely proportional to its thermal conductivity. In the current case, the U-pipes are installed closer to the pile wall; therefore, the influence of the thermal conductivity of the filling material on the pile thermal resistance should be less significant, as indicated by the results shown in Table 5.

Considering that the parametric 2D analysis allowed the estimation of the thermal conductivities of the backfill materials and the ground (Table 6), these thermal parameters were used for the application of the multipole model (an analytical method) to calculated the thermal resistance of P2, P3 and P4.

The results presented in Table 7 show that a lower pile thermal resistance was obtained for the pile filled with steel fiber grout, and similar R_b values was found for the piles filed with saturated sand and grout, as observed in Table 6. The higher value of the thermal conductivity of the steel fiber grout resulted in higher pile thermal resistance. This result agrees with the experimental results of fluid temperature variation measured during the tests, presented in Fig. 8.

Table 7. Thermal resistance estimated by multipole model.

Pile backfill	R_b (mK/W)
Saturated sand	0.082
Grout	0.078
Steel fiber grout	0.058

4.3.2. 3D Numerical model (for pile P1)

The 3D numerical analysis was developed to allow for better understanding of the convection effects in the pile filled with water. The model was validated by TRT-1 data by comparing the numerical and experimental results of the outlet pipe temperature variation. For the 3D simulation, an important step is to establish a convection model (laminar or turbulent flow) before starting the analysis.

Grashof, Rayleigh, and Prandtl numbers were calculated using the thermophysical properties of water at the initial temperature of the TRT (in the current case ~24°C). First, the numbers were scaled to the pile diameter and laminar flow was considered, as reported in Cao et al. [17], [67], and Spiltler et al. [68]. To validate the model, the outlet temperature variation from numerical analysis were compared with experimental measurements. The results did not fit the experimental data as expected (with a RMSE of 1.05).

Hadjadj et al. [67] showed by numerical investigation that the Nusselt number increases with Rayleigh number and with the GHE aspect ratio, and scaled these numbers with length. Arshad et al. [69] also scaled with GHE length, having correlated Nusselt and Rayleigh numbers by experimental tests. Therefore, the numerical analysis was repeated considering the depth of the pile as the length scale. In this case, both the Nusselt and Rayleigh numbers were higher than $10^{9,}$ which is the critical value and indicates that the flow regime is turbulent during the TRT.

To model the natural convection, turbulent non-Isothermal Flow was simulating using the k-ε Turbulence Model in COMSOL Multiphysics, with coupling from the Heat Transfer Module. The fluid was considered weakly compressible to take account of its density variations. The outlet temperature evolution from the numerical analysis was compared with measured data, as shown in Figure 15. The assumption of turbulent flow provides a better fit to the experimental measurements. The results show a good agreement between experimental and numerical data, with a RMSE of 0.20.

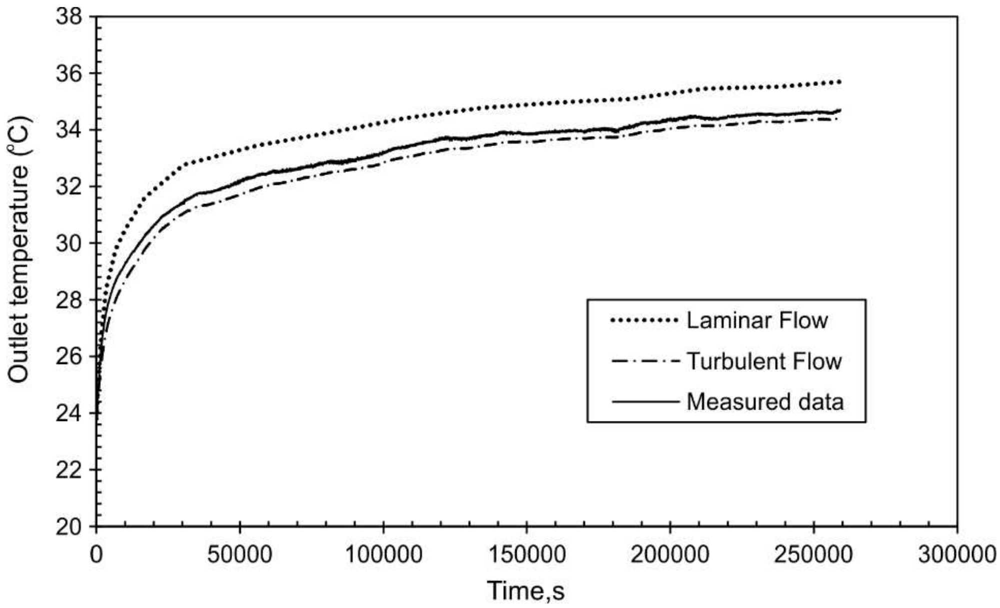

Figure 15.Comparison between measured outlet temperature and numerical results for laminar and turbulent flow

Additionally, the temperature variation, at the depths of the sensors installed in the pile, were compared with the numerical results. The curves are shown in Figure 16, with the calculated RMSE results. Temperature sensors were installed at 4, 12 and 20 m depth along the pile central axis, and at 2, 4, 8, 12, 16 and 20 m at the pile edge. The 3D numerical results are close to the experimental data.

The flow and velocity fields generated by the convection effects can be analyzed with the 3D numerical model. Coordinates X, Y and Z were adopted to help understand the convection mechanism. Figs. 17 and 18 show the velocity and temperature field of the pile for both XZ and YZ sections.

The results of section XZ show that the heated water rises mainly next to HDPE pipe region (Fig. 17) and in the central region while cooler water descends preferentially close to the pile edge (90 degrees from the HDPE pipe axis XZ) in section YZ (Fig. 18).

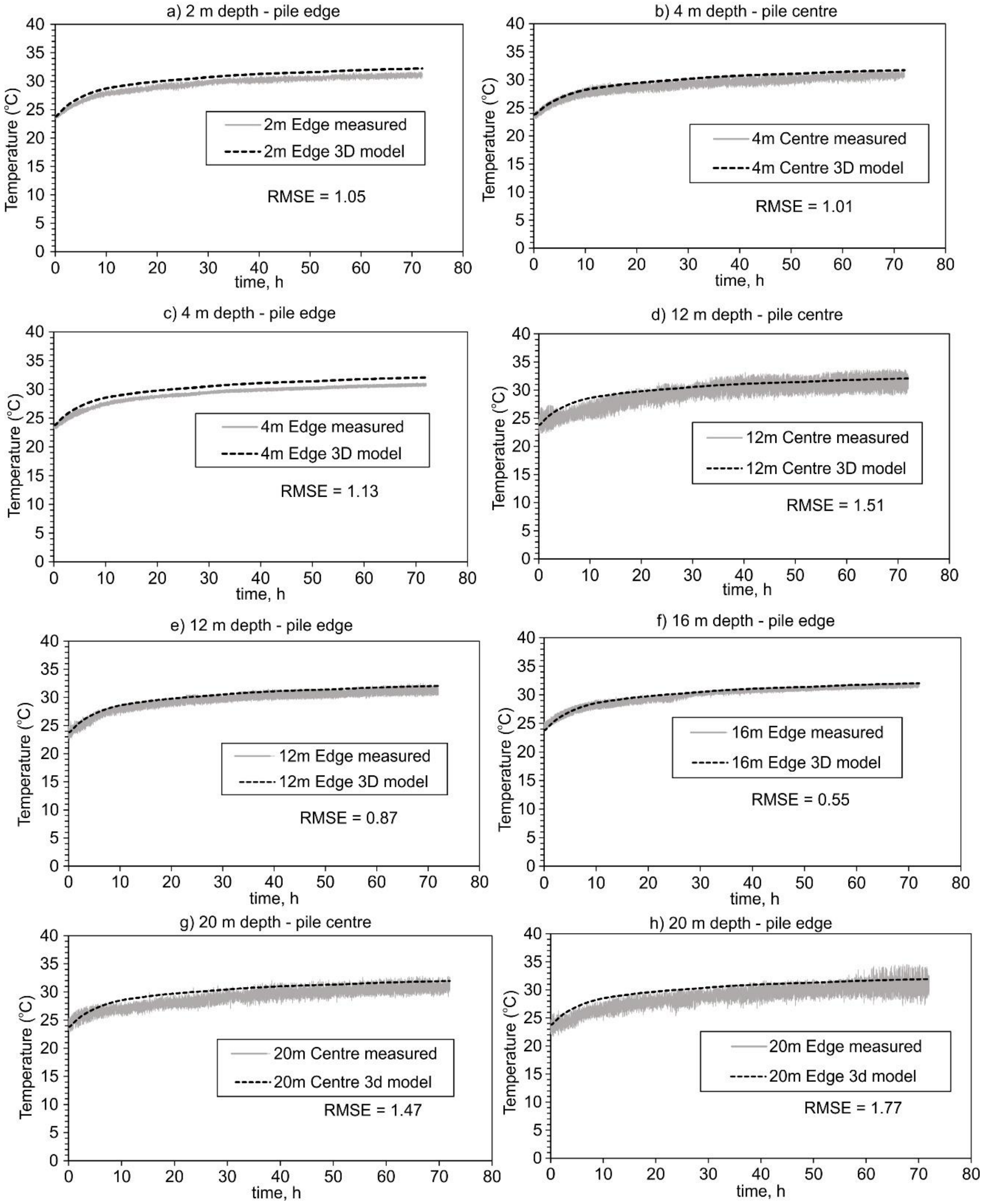

Figure 16. Measured vs. 3D numerical temperature variation at different depths in pile P1 (filled with water).

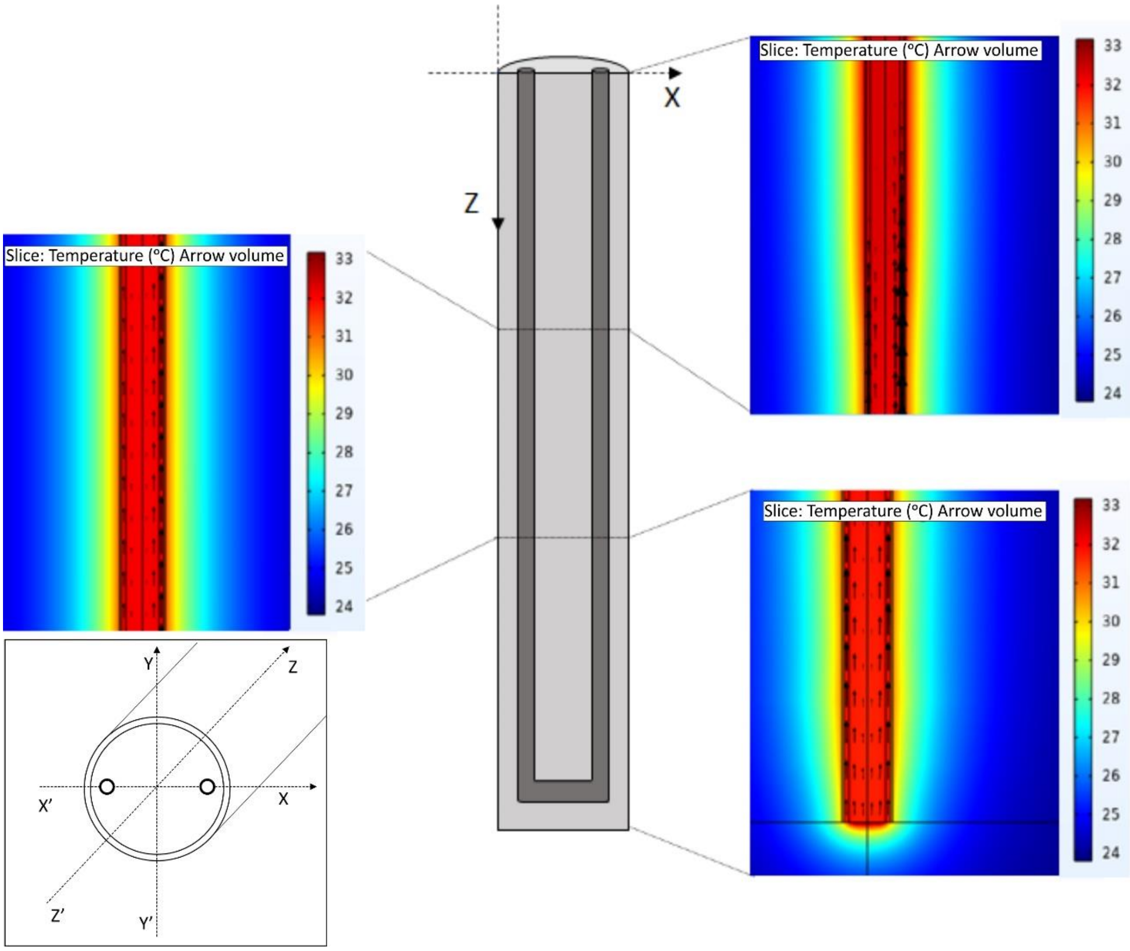

Figure 17. Velocity and temperature field generated by the 3D numerical model in the XZ cross section of the pile P1.

The intensity of the velocity field is proportional to the size of the arrows in the figures. In section XZ, there is a greater difference between the velocity field on the pile left and right side due to the temperature differential between the inlet and outlet pipes (Fig. 17). The difference decreases with depth and is almost the same for both sides at the pile base. In the section YZ, the convection effect is uniform along the pile. The results indicated that the pile length is the main direction of the convection turbulent flow, as also found by Hadjadj et al. [67], Spitler et al. [68], and Arshad et al. [69].

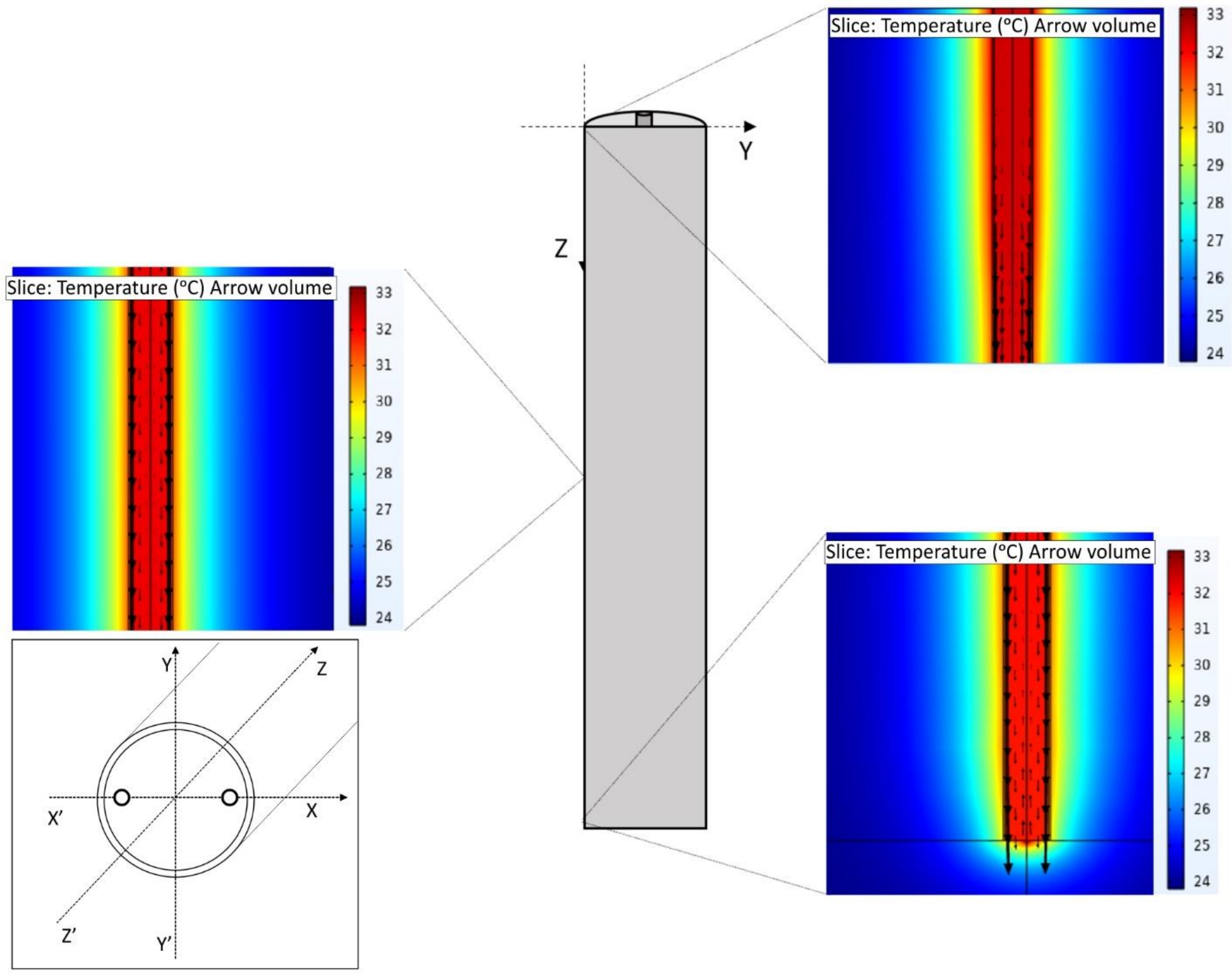

Figure 18. Velocity and temperature field generated by the 3D numerical model in the YZ cross section of the pile P1.

The pile thermal resistance of pile P1 (filled with water), determined by the outlet pipe and pile edge temperatures from numerical analysis, was 0.072 mK/W (with RMSE = 0.20). This value is lower than that obtained for piles P2 and P3 (filled with saturated sand or grout). According to Johnsson & Adl-Zarrabi [70], the convection effect in groundwater filled boreholes raises the effective thermal conductivity of the water in 2-3 times. Therefore, it was expected that the pile filled with water would present low thermal resistance due to buoyance-driven natural convection which increases the heat transfer.

5. Comparison of the results

Fig. 19 compare all results of pile thermal resistance obtained for the 4 types of pile tested in this study. The results of R_b obtained using ISLM, G-function and SCSM models are similar (~ 0.10 mK/W), and indicate that the pile backfill materials evaluated can provide similar heat transfer performance.

In contrast, as commented previously in the text, the analytical models do not consider the convection effects on the heat transfer performance of the pile filled with water, which was only simulated by a 3D numerical model. Therefore, as shown in Fig.19, the R_b value for the pile filled with water obtained from numerical simulation is ~ 30% lower (of 0.072 mK/W) compared to the values obtained from analytical solutions.

Fig. 19 also shows that the results obtained by the numerical and multipole models for piles P2, P3 and P4 (considering the thermal conductivity of backfill material obtained from 2D numerical simulation) provided lower results of pile thermal resistance compared to the other methods. These results are in accordance with the experimental results shown in Fig. 8, which indicates similar performance for the piles P2 and P3 (filled with sand and grout), and a slightly better performance for the pile P4 (filled with steel fiber grout).

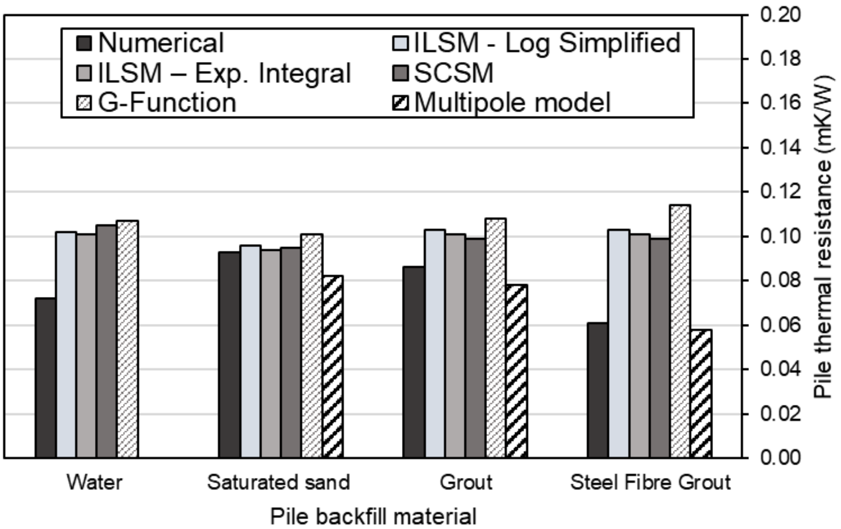

Figure 19. Results of pile thermal resistance obtained from analytical and numerical methods.

The results of R_b obtained by numerical simulations are compared with the backfill costs per pile length in Fig. 20. This figure indicates that the piles filled with saturated sand and water seem to be the optimum solutions when the backfill costs are taking into account. Depending on the original pile design prior to thermo-activation, it is possible that the use of either water or saturated sand as a filling material could lead to additional corrosion at the inside of the pipe, which could otherwise have been sealed for closed end pipes. In such cases, the structural performance of the piles would require additional design to confirm acceptable safety factors remain, or alternatively a more costly backfill option could be used instead.

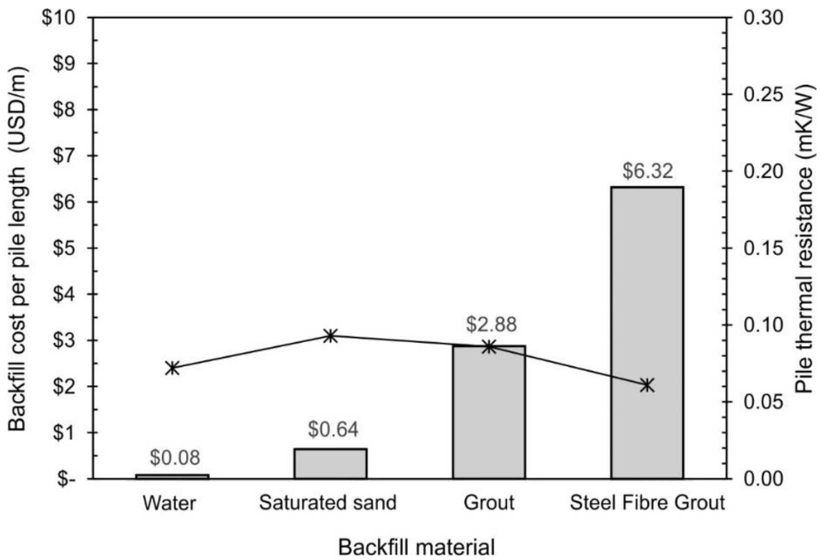

Figure 20. Results of pile thermal resistance (symbol and line) vs. backfill cost (bars) per pile length.

Additionally, the environmental impact of the backfill material cannot be disregarded. It is necessary to develop new solutions to mitigate the environmental impact and act to reduce CO2 emission. Cement represented 36% of the 7.7 gigatones (Gt) of CO2 global emission by construction activities in 2010 [71]. CO2 emissions from cement production is still high and it tends to increase with the rapid urbanization [71]. Cement production is difficult to decarbonize because even with use of low carbon energy supply, this does not eliminate the CO2 emission from calcination [72]. It is crucial to act to reduce the amount of cement in construction activities with alternative materials.

Therefore, to reduce the environmental impact, the use water or saturated sand can be environmental friendly alternatives to fill the energy piles, with similar thermal performance to those piles filled with grout materials. Moreover, the pile filled with water presented a slightly lower thermal resistance due to the convection mechanisms.

Finally, in terms of constructability performance, the four tested alternatives are similar. The pipe installation in closed end steel pile and the filling procedure are simple and rapid.

6. Conclusions

The motivation of the current study was to evaluate if low-cost and environmental-friendly alternatives of filling materials for steel pipe energy piles would provide heat transfer performance equivalent to the more expensive and less sustainable grout solutions. This research was conducted to provide results to be used for the design of a GSHP system for a real case of building. For this purpose, in situ thermal response tests were conducted on 4 steel pipe piles filled with different materials (water, saturated sand, grout, and grout + steel fibers) at a test site in Sao Paulo city, Brazil. Analytical and numerical techniques were employed to determine the ground thermal conductivity at the test site, and the thermal resistance of the tested piles. The latter is the main parameter used in this work to evaluate and compare the four solutions studied. The main conclusions are:

1. The ground thermal conductivity and pile thermal resistance of 244mm diameter steel pipe energy piles with high aspect ratio (AR of ~ 94) can be estimated from TRT's with duration of 72 hours using a simple and rapid ISLM analytical solution. However, in one case conductivity and resistance were overestimated during heat injection, illustrating the importance of including a recovery phase for independent determination of conductivity.
2. For the pile filled with water, the analytical solutions tested in this study are not appropriated because they do not consider the existence of convection effects.

3. A numerical 3D simulation performed for the pile filled with water illustrated the convention mechanism along the pile length, and showed a value of pile thermal resistance 30% lower than the results found by analytical solutions.
4. The numerical analyses showed that the thermal resistance of the steel pile filled with grout is about 20% greater than that of the pile filled with water, and are similar to that of the pile filled with saturated sand.
5. The most economic energy piles alternatives tested in this study, using piles filled with water or saturated sand, given better or equivalent thermal performance compared to conventional grout solutions. The use of grout with steel fibers provided a slightly lower pile thermal resistance compared to the case filled with water, however the total costs of this alternative are much higher compared to the other tested backfill materials. Additionally, the construction of pipe energy piles filled with water or saturated sand contributes to a lower CO2 emission compared to the cases of piles with backfill materials using cement.

Acknowledgements

The authors gratefully acknowledge the financial support given by TUPER S/A, the Center for Innovation in Sustainable Construction, CICS/USP, the State of São Paulo Research Foundation - FAPESP (Process 2014/14496–0), the National Council for Scientific and Technological Development - CNPQ for the financial support (Process 310881/2018-8), and the Coordination of Improvement of Higher Education Personnel — CAPES for granting the doctoral scholarship of the first author (Process: CAPES-PRINT: 88887.465711/2019-00).

Data Statement

The data from the field experiments presented in this study are available via contact with the corresponding author.

References

[1] IEA, Tacking Buildings, Paris, France, 2019. https://www.iea.org/reports/tracking-buildings (accessed 13 March 2022).

[2] Ciancio, V., Falasca, S., Golasi, I., de Wilde, P., Coppi, M., de Santoli, L., & Salata, F, 2019. Resilience of a building to future climate conditions in three European cities. Energies, 12 (23), 4506. https://doi.org/10.3390/en12234506.

[3] de Oliveira, C. C., Rupp, R. F., & Ghisi, E., 2021. Influence of environmental variables on thermal comfort and air quality perception in office buildings in the humid subtropical climate zone of Brazil. Energy and Buildings, 243, 110982. https://doi.org/10.1016/j.enbuild.2021.110982.

[4] Empresa, D. P. E, 2018. Uso de ar condicionado no setor residencial brasileiro: perspectivas e contribuições para o avanço em eficiência energética. 2010. https://www.epe.gov.br/pt/publicacoes-dados-abertos/publicacoes/balanco-energetico-nacional-2018 (acessed 10 March 2022).

[5] Michels-Brito, A., Rodriguez, D. A., Junior, W. L. C., & de Souza Vianna, J. N. (2021). The climate change potential effects on the run-of-river plant and the environmental and economic dimensions of sustainability. Renewable and Sustainable Energy Reviews, 147, 111238. https://doi.org/10.1016/j.rser.2021.111238

[6] Loveridge, F. and Powrie, W. Temperature response functions (G-functions) for single pile heat exchangers. Energy, 57 (2013) 554-564. https://doi.org/10.1016/j.energy.2013.04.060.

[7] Sutman, M., Olgun, C. G., & Brettmann, T. Full-scale field testing of energy piles. In IFCEE (2015) 1638-1647. https://doi.org/10.1061/9780784479087.148.

[8] Laloui, L. Loria, A. R. Analysis and design of energy geostructures: theoretical essentials and practical application. Academic Press, 2019.

[9] Brandl, H. Energy foundations and other thermo-active ground structures. Géotechnique, 56 (2) (2006) 81-122. https://doi.org/10.1680/geot.2006.56.2.81.

[10] Henderson, H. I., Carlson, S. W., & Walburger, A. (1998). North American monitoring of a hotel with room size GSHPS. In Proc., IEA 1998 room size heat pump conference.

[11] Ren, L. W., Xu, J., Kong, G. Q., & Liu, H. L. Field tests on thermal response characteristics of micro-steel-pipe pile under multiple temperature cycles. Renewable Energy, 147 (2020) 1098-1106. https://doi.org/10.1016/j.renene.2019.09.084.

[12] Miyara, A., Tsubaki, K., Inoue, S., & Yoshida, K. Experimental study of several types of ground heat exchanger using a steel pile foundation. Renewable Energy, 36 (2) (2011) 764-771. https://doi.org/10.1016/j.renene.2010.08.011.

[13] Morino, K., & Oka, T. Study on heat exchanged in soil by circulating water in a steel pile. Energy and Buildings, 21(1) (1994) 65-78. https://doi.org/10.1016/0378-7788(94)90017-5.

[14] Nagano, K. Thermal characteristics of steel foundation piles as ground heat exchangers. In Proceedings of 8th International Energy Agency Heat Pump Conference 2005, Las Vegas, USA.

[15] Katsura, T., Nakamura, Y., Okawada, T., Hori, S., & Nagano, K. Field test on heat extraction or injection performance of energy piles and its application. In Effstcok 2009. The 11th International Conference on Energy Storage (Vol. 146).

[16] Huang, J., McCartney, J. S., Perko, H., Johnson, D., Zheng, C., & Yang, Q. (2019). A novel energy pile: The thermo-syphon helical pile. Applied Thermal Engineering, 159, 113882.

[17] Cao, Z., Zhang, G., Liu, Y., Zhao, X., Li, C. Influence of backfilling phase change material on thermal performance of precast high-strength concrete energy pile. Renewable Energy, 184 (2022) 374-390. https://doi.org/10.1016/j.renene.2021.11.100

[18] Romanoff, M. 1972. NBS papers on underground corrosion of steel piling, 1962–1971. Vol. 127. National Bureau of Standards, Gaithersburg, Md.

[19] Ohsaki, Y. 1982. Corrosion of steel piles driven in soil deposits. Soils and Foundations, 22(3): 57–76. doi:10.3208/sandf1972.22.3_57.

[20] Wong, I.H., and Law, K.H. 1999. Corrosion of steel H piles in decomposed granite. Journal of Geotechnical and Geoenvironmental Engineering, ASCE, 125(6): 529–532. doi:10.1061/(ASCE)1090-0241(1999)125:6(529).

[21] Decker, J.B., Rollins, K.M., and Ellsworth, J.C. 2008. Corrosion rate evaluation and prediction for piles based on long-term field performance. Journal of Geotechnical and Geoenvironmental Engineering, ASCE, 134(3): 341–351. doi:10.1061/(ASCE)1090-0241(2008)134:3(341).

[22] Ding, L. 2019. Corrosion behavior of H-pile steel in different soils. Doctoral dissertation, Clemson University, Clemson, S.C.

[23] FinnRA, 2000. Steel Pipe Piles, Helsinki.

[24] Grand, B. A. (1970). Types of piles: their characteristics and general use. Highway Research Record, (333).

[25] California Department of Transportation. 2021. Corrosion Guidelines. California Department of Transportation, Division of Engineering Services Materials Engineering and Testing Services Corrosion Branch, Sacramento, Calif.

[26] Aguirre, D. A., Kowalsky, M. J., Nau, J. M., Gabr, M., & Lucier, G. Seismic performance of reinforced concrete filled steel tube drilled shafts with inground plastic hinges. Engineering Structures, 165 (2018) 106-119. https://doi.org/10.1016/j.engstruct.2018.03.034.

[27] Yoon, S., Lee, S. R., Xue, J., Zosseder, K., Go, G. H., & Park, H. Evaluation of the thermal efficiency and a cost analysis of different types of ground heat exchangers in energy piles. Energy Conversion and Management, 105 (2015) 393-402. https://doi.org/10.1016/j.enconman.2015.08.002.

[28] Hamada, Y., Saitoh, H., Nakamura, M., Kubota, H., & Ochifuji, K. Field performance of an energy pile system for space heating. Energy and Buildings, 39(5) (2007) 517-524. https://doi.org/10.1016/j.enbuild.2006.09.006

[29] Guo, Y., Zhang, G., & Liu, S. (2018). Investigation on the thermal response of full-scale PHC energy pile and ground temperature in multi-layer strata. Applied Thermal Engineering, 143 (2018) 836-848. https://doi.org/10.1016/j.applthermaleng.2018.08.005

[30] Takeda, T., Ishiguro, S., Yoda, O., & Okubo, H. Thermal performance of ground source heat pumps that use direct expansion method using foundation pile. In International Heat Transfer Conference Digital Library, 2018. Begel House Inc.

[31] Keltbray, 2022. Redefining sustainable construction - HIPER® Pile. Brochure https://issuu.com/keltbraygroup/docs/keltbrayhiper__pile?fr=sNTQ0ZTIxNjEzMzU. (acessed 20 June 2022).

[32] Murari, M. C. F Study of the behaviour of steel pipe energy piles for shallow geothermal heat exchange, 250 p. Thesis (Doctorate) – São Carlos School of Engineering, University of São Paulo, São Carlos, 2022.

[33] White, D., Finlay, T., Bolton, M., & Bearss, G. (2002). Press-in piling: Ground vibration and noise during pile installation. Geotechnical Special Publication, 1, 363-371.

[34] Hashimoto, M., Hashimoto, O., & Nishizawa, S. (1994). Rotary Penetration Steel Pipe Pile (Drill Pile) Method:—New Low-Noise, Low-Vibration Piling Method—. Soils and foundations, 34(1), 119-125.

[35] Ishihara, Y., Haigh, S., & Bolton, M. (2015). Estimating base resistance and N value in rotary press-in. Soils and Foundations, 55(4), 788-797.

[36] Bolton, M. D., Kitamura, A., Kusakabe, O., & Terashi, M. (2021). New Horizons in Piling: Development and Application of Press-in Piling. CRC Press.

[37] Loveridge, F., Powrie, W. 2D thermal resistance of pile heat exchangers. Geothermics, 50, (2014), 122-135. https://doi.org/10.1016/j.geothermics.2013.09.015

[38] You, S., Cheng, X., Guo, H., & Yao, Z. 2014. In-situ experimental study of heat exchange capacity of CFG pile geothermal exchangers. Energy and buildings, 79, 23-31.

[39] Vieira, A., Maranha J., Christodoulides P., Alberdi-Pagola, M., Loveridge, F., Nguyen, F., et al., 2017. Characterisation of ground thermal and thermo-mechanical behaviour for shallow geothermal energy applications. Energies 10 (12), 2044. https://doi.org/10.3390/en10122044.

[40] Ingersoll L. R., Zobel, O. J., Ingersoll, A. C. Heat conduction with engineering and geological applications. 3rd ed., 1954. New York: McGraw-Hill.

[41] Carslaw, H.S., Jaeger, J.C.Conduction of Heat in Solids. Oxford University Press, New York, NY, USA, 1959, 510 p.

[42] Poppei, J., Péron, H., Silvani, C., Steinmann, G., Laloui L., Wagner, R., Lochbuhler, T., Rohner, E., 2008. Innovative Improvements of Thermal Response Tests Final Report. Swiss Federal Office of Energy, p. 1-34.

[43] Eskilson, P. Thermal analysis of heat extraction boreholes. Doctoral Thesis, 1987. Lund Inst. of Tech. (Sweden). Dept. of Mathematical Physics

[44] Loveridge, F., Holmes, G., Powrie, W., & Roberts, T.. Thermal response testing through the Chalk aquifer in London, UK. Proceedings of the Institution of Civil Engineers-Geotechnical Engineering, 166 (2), (2013) 197-210. https://doi.org/10.1680/geng.12.00037.

[45] Man, Y., Yang, H., Diao, N., Liu, J. and Fang, Z., 2010. A new model and analytical solutions for borehole and pile ground heat exchangers. International Journal of Heat and Mass Transfer, 53 (2010) 2593-2601. https://doi.org/10.1016/j.ijheatmasstransfer.2010.03.001.

[46] Carslaw, H. S, Jaeger, J. C. Operational Method in Applied Mathematics, 1947. 2nd Edition, chapter 6. Oxford University.

[47] Marcotte, D., & Pasquier, P. On the estimation of thermal resistance in borehole thermal conductivity test. Renewable energy, 33 (2008) 2407-2415. https://doi.org/10.1016/j.renene.2008.01.021.

[48] Loveridge, F., Low, J., & Powrie, W. Site investigation for energy geostructures. Quarterly Journal of Engineering Geology and Hydrogeology, 50 (2017) 158-168. https://doi.org/10.1144/qjegh2016-027.

[49] Hahn, D. W., & Özisik, M. N. Heat conduction. John Wiley & Sons, 2012.

[50] Hamdhan, I. N., & Clarke, B. G., 2010. Determination of thermal conductivity of coarse and fine sand soils. In Proceedings of World Geothermal Congress (pp. 1-7).

[51] Kim, D., Kim, G., Kim, D., & Baek, H., 2017. Experimental and numerical investigation of thermal properties of cement-based grouts used for vertical ground heat exchanger. Renewable Energy, 112 (2017) 260-267.

[52] Rees, S.W., Adjali, M.H., Zhou, Z., Davies, M. and Thomas, H.R. Ground heat transfer effects on the thermal performance of earth-contact structures. Renewable and Sustainable Energy Reviews, 4(3) (2000) 213-265. https://doi.org/10.1016/S1364-0321(99)00018-0.

[53] Hellstrom, G., 1991. Ground heat Storage., Thermal analysis of duct storage Systems, Theory. Department of Mathermatical Physics, University of Lund, Sweden.

[54] Benner J., Claesson, J., Hellstrom G., 1987. Multipole method to compute the conductive heat flow to and between pipes in a composite cylinder. Notes on heat transfer 3-1987. University of Lund, Department pf Building Technology and Mathematical Physics. Lund, Sweden

[55] Javed, S., & Spitler, J. D. Calculation of borehole thermal resistance. In Advances in ground-source heat pump systems, 2016, pp. 63-95. Woodhead Publishing.

[56] Lamarche, L., Kajl, S., Beauchamp,B., 2010. A review of methods to evaluate borehole thermal resistance in geothermal heat pump systems. Geotermics 39, 187 – 200.

[57] Liao, Q., Zhou, C., Cui, W., Jen, T.C., 2012. New correlations for thermal resistances of vertical single U-tube ground heat exchanger. Journal of Thermal Science and Engineering Applications 4 (3), 031010. https://doi.org/10.1115/1.4006516.

[58] Go, G.H., Lee, S.R., Yoon, S., Park, H., Park, S., 2014. Estimation and experimental validation of borehole thermal resistance. KSCE Journal of Civil Engineering 18 (4), 992- 1000. https://doi.org/10.1007/s12205-014-0454-x

[59] Todorov, O., Alanne, K., Virtanen, M., & Kosonen, R. Different Approaches for Evaluation and Modeling of the Effective Thermal Resistance of Groundwater-Filled Boreholes. Energies, 14 (2021) 6908. https://doi.org/10.3390/en14216908

[60] Gustafsson, A. M., Westerlund, L.,2011. Heat extraction thermal response test in groundwater-filled borehole heat exchanger – Investigation of the borehole thermal resistance. Renew Energy 36 (2011) 2388-2394. https://doi.org/10.1016/j.renene.2010.12.023.

[61] Lieberl, H. T., Javed, S., Vistnes, G. Multi-injection rate thermal response test with forced convection in groundwater-filled borehole in hard rock. Renew. Energy, 48 (2012) 263-268. https://doi.org/10.1016/j.renene.2012.05.005

[62] Alberdi-Pagola, M., Poulsen, S. E., Loveridge, F., Madsen, S., & Jensen, R. L. Comparing heat flow models for interpretation of precast quadratic pile heat exchanger thermal response tests. Energy, 145 (2018) 721-733. https://doi.org/10.1016/j.energy.2017.12.104.

[63] COMSOL Multiphisics. COMSOL Reference Manual (Version 5.4), 2018.

[64] Churchill, S. W. Friction-factor equation spans all fluid-flow regimes, 1977.

[65] Terzaghi, K., Peck, R. B., & Mesri, G. Soil mechanics in engineering practice. John Wiley & Sons, 1996.

[66] Cecinato, F., & Loveridge, F. A. Influences on the thermal efficiency of energy piles. Energy, 82 (2015) 1021-1033. https://doi.org/10.1016/j.energy.2015.02.001.

[67] Hadjadj A., Maamir S., Zeghmati B. A new study of laminar natural convection in two concentric vertical cylinders. Heat Mass transfer 1999; 35 (1999) 113-21.

[68] Spitler, J. D.; Javed, S.; Ramstad, R. K. Natural convection in groundwaterfilled boreholes used as ground heat exchangers. Applied Energy, v. 164, (2016) 352-365. https://doi.org/10.1016/j.apenergy.2015.11.041.

[69] Arshad, M., Inayat, M. H., Chughtai, I. R. (2011). Experimental study of natural convection heat transfers from an enclosed assembly of thin vertical cylinders. Applied Thermal Engineering, 31(2011) 20-27. https://doi.org/10.1016/j.applthermaleng.2010.07.031.

[70] Johnsson, J., Adl-Zarrabi, B., 2019. Modelling and evaluation of groundwater filled boreholes subjected to natural convection. Appl. Energy, 253, 113555. https://doi.org/10.1016/j.apenergy.2019.113555.

[71] Bajželj, B., Allwood, J. M. & Cullen, J. M., 2013. Designing climate change mitigation plans that add up. Environ. Sci. Technol. 47 (2013) 8062–8069. https://doi.org/10.1021/es400399h.

[72] Habert, G., Miller, S. A., John, V. M., Provis, J. L., Favier, A., Horvath, A., & Scrivener, K. L. Environmental impacts and decarbonisation strategies in the cement and concrete industries. Nature Reviews Earth & Environment, 1(2020) 559-573. https://doi.org/10.1038/s43017-020-0093-3.